BIT-AWARE RANDOMIZED RESPONSE FOR LOCAL DIFFERENTIAL PRIVACY IN FEDERATED LEARNING

Anonymous authors
Paper under double-blind review

ABSTRACT

In this paper, we develop **BitRand**, a bit-aware randomized response algorithm, to preserve local differential privacy (LDP) in federated learning (FL). We encode embedded features extracted from clients' local data into binary encoding bits, in which different bits have different impacts on the embedded features. Based upon that, we randomize all the bits to preserve LDP with three key advantages: **(1)** Bit-aware: Bits with a more substantial influence on the model utility have smaller randomization probabilities, and vice-versa, under the same privacy protection; **(2)** Dimension-elastic: Increasing the dimensions of embedded features, gradients, model outcomes, and training rounds marginally affect the randomization probabilities of binary encoding bits under the same privacy protection; and **(3)** LDP protection is achieved for both embedded features and labels with tight privacy loss and expected error bounds ensuring high model utility. Extensive theoretical and experimental results show that our BitRand significantly outperforms various baseline approaches in text and image classification.

1 INTRODUCTION

Recent data privacy and security regulations (GDPR, 2018; Regulation, 2018; Cybersecurity Law, 2016) pose major challenges in collecting and using personally sensitive data in different places for machine learning (ML) applications. Federated Learning (FL) (McMahan et al., 2017; Kairouz et al., 2019) is a promising way to address these challenges, enabling clients to jointly train ML models by sharing and aggregating gradients computed from clients' local data through a coordinating server for model updates. However, recent attacks (Zhu et al., 2019; Y. et al., 2021; Zhao et al., 2020a) have shown that clients' training samples, each of which includes an input x and a ground-truth label y_x, can be extracted from the shared gradients. These attacks underscore the implicit privacy risk in FL.

Our main goal is to provide a strong guarantee that the shared gradients protect the privacy of clients' local data without undue sacrifice in model utility. Local differential privacy (LDP) has emerged as a crucial component in various FL applications (Yang et al., 2019; Kairouz et al., 2019). To achieve our goal, we focus on preserving LDP in cross-device FL, i.e., in which clients jointly train an FL model (Kairouz et al., 2019).

In cross-device FL, existing LDP-preserving approaches can be categorized into three lines: Clients **(1)** add noise into local gradients derived from their local training samples, e.g., using Gaussian mechanism (Abadi et al., 2016), to protect membership information at the training sample level with DP guarantees (Zheng et al., 2021; Dong et al., 2019; Malekzadeh et al., 2021; Geyer et al., 2017; Huang et al., 2020), **(2)** add noise to local gradients using Randomized Response (RR) mechanisms to protect the values of the local gradients with LDP guarantees (Sun et al., 2021; Liu et al., 2020; Zhao et al., 2020b; Wang et al., 2019a), and **(3)** add noise into each training sample, e.g., embedded features and labels, using RR mechanisms to protect the value of each training sample with LDP guarantees (Arachchige et al., 2019; Lyu et al., 2020a), then the clients use LDP-preserved training samples to derive local gradients. For all three approaches, in each training round, clients send DP or LDP-preserved local gradients to the coordinating server for model updates, which will be sent back to the clients for the next training round.

In this paper, we focus on protecting clients' training data at the value level with LDP guarantees. Existing RR mechanisms to preserve LDP in FL suffer from the *curse of privacy composition*, in which excessive privacy budgets are consumed proportionally to the large dimensions of input or embedded features (Arachchige et al., 2019), gradients (Zhao et al., 2020b; Wang et al., 2019a), and training rounds (Zhao et al., 2020b; Wang et al., 2019a), causing loose privacy protection or inferior model accuracy (Wagh et al., 2021).

Addressing the curse of privacy composition is non-trivial. Existing approaches, such as anonymizers (assumed to be trusted), i.e., shuffler (Erlingsson et al., 2019; Sun et al., 2021; L. et al., 2020; Wang et al., 2019b; Cheu et al., 2019; Balle et al., 2019) or anonymity approaches (e.g., faking source IP, VPN, Proxy, etc. (Sun et al., 2021; Cormode et al., 2018)), and dimension reduction (Liu et al., 2020; Zhao et al., 2020b; Shin et al., 2018; Xu et al., 2019), mitigate the problem but also have limitations. In the real world, it is possible that the anonymizers can either be compromised or collude with the coordinating server to extract sensitive information from observing LDP-preserved local gradients (Erlingsson et al., 2019). Meanwhile, applying RR mechanisms on reduced sets of embedded features or gradients using dimension reduction techniques can work well with lightweight models, such as logistic regression and SVM (Liu et al., 2020; Zhao et al., 2020b; Wang et al., 2019a). However, it is challenging for these techniques to achieve good model utility under tight LDP guarantees given complex models and tasks, such as DNNs, since the dimensions of reduced embedded features, gradients, and training rounds still need to be sufficiently large (Zhao et al., 2020b; Liu et al., 2020).

Hence, the curse of privacy composition in preserving LDP by applying RR mechanisms in FL remains a largely open problem. Orthogonal to this, preserving LDP to protect ground-truth labels y_x in FL has not been well-studied. Two known approaches for centralized training are 1) injecting Laplace noise into the labels (Phan et al., 2020) and 2) applying RR mechanisms on the labels to achieve DP at the label level (Ghazi et al., 2021). However, centralized training in Ghazi et al. (2021) has not been designed for FL with LDP guarantees since they require centralized and trusted databases. The model utility in Phan et al. (2020) is notably affected by the number of model outcomes.

Key Contributions. To mitigate the curse of privacy composition and optimize the trade-off between privacy and model utility, our paper is structured around the following contributions:
1) We propose **BitRand**, which is a combination of a novel *bit-aware* f-**RR** mechanism and $label$-**RR** mechanism, to preserve LDP at both levels of embedded features and labels in FL. In f-**RR**, we encode embedded features (extracted from x) into a binary-bit string, which will be adaptively randomized such that bits with *a more substantial impact* on model utility will have *smaller randomization probabilities* and vice-versa under the same privacy budget. To preserve LDP on y_x, we develop a generalized randomization, in which the probability of randomizing label y_x from one to another class is a function of the number of model outcomes C. By doing that, we can optimize the trade-off between model utility and privacy loss with significantly tighter expected error bounds.
2) By incorporating sensitivities of binary encoding bits into a generalized privacy loss bound, we show that increasing the dimensions of embedded features r, encoding bits l, and model outcomes C marginally affect the randomization probabilities in BitRand under the same privacy budget. This *dimension-elastic* property is crucial to evade the curse of privacy composition by retaining a high value of data transmitted correctly through our randomization given large dimensions of r, l, and C.
3) These bit-aware and dimension-elastic properties allow us to work with complex models and tasks with formal LDP guarantees for training samples (x, y_x) while retaining high model utility. Extensive theoretical analysis and experimental results conducted on fundamental FL tasks, i.e., text and image classification, using benchmark datasets and our collected Security and Exchange Commission financial contract dataset show that our BitRand significantly outperforms a variety of baseline approaches in terms of model utility under the same privacy budget.

2 Background

LDP-preserving mechanisms (Erlingsson et al., 2014; Duchi et al., 2018; Wang et al., 2017; Acharya et al., 2019; Bassily & Smith, 2015) generally build on the ideas of randomized response (Warner, 1965), which was initially introduced to allow survey respondents to provide their correct inputs while maintaining their confidentiality. ϵ-LDP is presented as follows:

Definition 1. *ϵ-LDP. A randomized algorithm $\mathcal{M}$ fulfills ϵ-LDP, if for any two inputs x and x', and for all possible outputs $\mathcal{O} \in Range(\mathcal{M})$, we have: $Pr[\mathcal{M}(x) = \mathcal{O}] \leq e^{\epsilon} Pr[\mathcal{M}(x') = \mathcal{O}]$, where ϵ is a privacy budget and $Range(\mathcal{M})$ denotes every possible output of the algorithm $\mathcal{M}$.*

The privacy budget ϵ controls the amount by which the distributions induced by inputs x and x' may differ. A smaller ϵ enforces a stronger privacy guarantee. We revisit RR mechanisms for LDP preservation in **Appendix A**. Our approach is a binary encoding-based approach, similar to (Arachchige et al., 2019; Lyu et al., 2020a), since it has the potential to overcome the curse of privacy composition. In binary encoding, x is converted into an l-bit vector v consisting of 1 sign bit, m bits for the integer part, and $l{-}m{-}1$ bits for the fraction part (Figure 1), as follows:

$$\forall i \in [0, l-1] : v_i = \lfloor 2^{i-m} |x| \rfloor \mod 2 \tag{1}$$

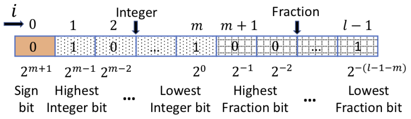

Figure 1: Binary encoding.

Each bit in v is randomized by applying a RR mechanism, e.g., (Erlingsson et al., 2014; Bassily & Smith, 2015; Wang et al., 2017), to generate a perturbed l-bit vector v', which preserves LDP. However, in our theoretical reassessment (**Appendices I** and **J**), directly applying RR mechanisms on binary encoded vectors as in existing mechanisms, i.e., LATENT (Arachchige et al., 2019) and OME (Lyu et al., 2020a), consumes huge privacy budgets since each binary encoding bit cannot be treated as a bit in a hash. Each binary encoding bit i has a different sensitivity, i.e., $\Delta_i = 2^{m-i}$ for the integer and fraction parts or $\Delta_i = 2^{m+1}$ for the sign bit (**Lemma 1**), compared with a bit B_i in a hash, i.e., $\forall B_i : \Delta_{B_i} = 1$. Our mechanism does not suffer from this problem, thanks to our bit-aware randomization in binary encoding (**Theorem 2**).

3 BitRand Algorithm

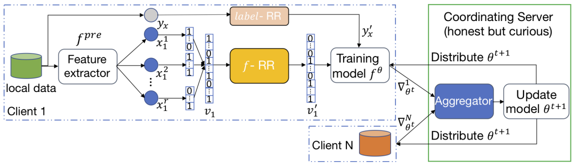

Figure 2: Federated Learning with BitRand Algorithm.

Let us now present our FL setting, threat model, and BitRand algorithm (Figure 2 and Alg. 1, Appendix B), and privacy guarantees. Then, we will show that our algorithm is dimension-elastic and the ability to optimize the randomization probabilities with expected error bounds in our theoretical analysis.

Federated Learning Given N clients, each client $u \in [1, N]$ has a set of training samples $D_u = \{(x, y_x)\}_{n_u}$ where $x \in \mathbb{R}^d$ is the input features, and its associated ground-truth label $y_x \in \mathbb{Z}^C$ is one-hot encoded with C categorical model outcomes $\{y_{x,1}, \dots, y_{x,C}\}$, and n_u is the number of training samples. In a pre-processing step, each client u extracts r numerical embedded features from x, denoted e_x, by using a pre-trained model f^{pre}. In practice, f^{pre} could be trained on large-scale and publicly available datasets without introducing any extra privacy cost to the clients' local data (He et al., 2016; Devlin et al., 2018). N clients jointly train the model $f^\theta : \mathbb{R}^r \rightarrow \mathbb{R}^C$ by minimizing a loss function $\mathcal{L}\big(f^\theta(e_x), y_x\big)$ on their local training samples in D_u that penalizes mismatching between the prediction $f^\theta(e_x)$ and the ground-truth label y_x, given the model's parameters θ. In each training round t, each client u receives the most updated model parameters θ^t from the coordinating server and then computes local gradients $\triangledown^u_{\theta_t} = \sum_{(v_x, y_x) \in D_u} \triangledown_{\theta_t} \mathcal{L}(f(e_x), y_x)/n_u$, which are sent to the coordinating server for aggregating and model updating: $\theta_{t+1} = \theta_t - \eta_t \sum_{u \in [1,N]} \triangledown^u_{\theta_t}/N$.

Threat Model. The coordinating server strictly follows the training procedure but curious about the training data D_u. This is a practical threat model in the real world since service providers always aim at providing the best services to the clients (Haeberlen et al., 2011; Truex et al., 2019; Lyu et al., 2020b). Given the observed gradients $\triangledown^u_{\theta_t}$, the coordinating server can extract the clients' data $\{e_x, y_x\}_{n_u}$ by using recently developed attacks (Carlini et al., 2020; Fredrikson et al., 2015). In a defense-free environment, $\{e_x, y_x\}_{n_u}$ can be used to infer the sensitive training data $D_u = \{(x, y_x)\}_{n_u}$ using the pre-trained model f^{pre}, since $f^{pre}(x) = e_x$ (Song & Raghunathan, 2020). This poses a severe privacy risk to the sensitive data D_u.

BitRand Algorithm. To protect the sensitive training data D_u against the threat model, in our algorithm, we preserve LDP on both embedded features e_x and labels y_x.

Each of the r embedded features in e_x is encoded into l binary bits following Eq. 1. Binary encoded features are concatenated together into a vector v_x consisting of rl binary bits to represent the embedded features e_x (Alg. 1, line 16). Each bit $i \in [0, rl - 1]$ in v_x is randomized by our ***f*-RR** mechanism (Alg. 1, line 17) with a *bit-aware term* $\frac{i\%l}{l}$ optimizing randomization probabilities:

$$(f\text{-RR mechanism}) \quad \forall i \in [0, rl-1] : P(v'_x(i) = 1) = \begin{cases} p_X = \dfrac{1}{1 + \alpha \exp(\frac{i\%l}{l}\epsilon_X)}, & \text{if } v_x(i) = 1 \\[2ex] q_X = \dfrac{\alpha \exp(\frac{i\%l}{l}\epsilon_X)}{1 + \alpha \exp(\frac{i\%l}{l}\epsilon_X)}, & \text{if } v_x(i) = 0 \end{cases} \tag{2}$$

where $v_x(i) \in \{0, 1\}$ is the value of v_x at the bit i, v'_x is the perturbed vector created by randomizing all the bits in v_x, ϵ_X is a privacy budget, and α is a parameter bounded in Theorem 2. From Eq. 2, we also have that $P(v'_x(i) = 0) = 1 - p_X$ if $v_x(i) = 1$, and $P(v'_x(i) = 0) = 1 - q_X$ if $v_x(i) = 0$. We use the bit-aware term $\frac{i\%l}{l}$ to indicate the location of bit i, which is associated with the sensitivity of the bit at that location, in its l-bit binary encoded vector among rl concatenated binary bits.

One of the key differences between our mechanism and existing works (Sun et al., 2021; Zhao et al., 2020b; Wang et al., 2019a; Liu et al., 2020; Arachchige et al., 2019; Lyu et al., 2020a) is the bit-aware randomization probabilities. By introducing the bit-aware term $\frac{i\%l}{l}$, we are able to: 1) Derive significantly tighter privacy loss and expected error bounds compared with existing approaches (**Sections 4 and 5**); and 2) Adaptively control the randomization probabilities across bits, such that bits with a *stronger influence* on the model utility, e.g., sign bits and integer bits, have *smaller randomization probabilities* q_X, and vice-versa (**Section 5**). These advantages are crucial to evade the curse of privacy composition enabling us to work with complex tasks and models (**Section 6**).

In addition, inspired by the LabelDP (Ghazi et al., 2021), we randomize y_x using the following $label$-**RR** mechanism (Alg. 1, line 18):

$$(label\text{-RR mechanism}) \quad P(y'_x = \bar{y}_x) = \begin{cases} p_Y = \dfrac{\exp(\beta)}{1+\exp(\beta)}, & \text{if } \bar{y}_x = y_x \\ q_Y = \dfrac{1}{(1+\exp(\beta))(C-1)}, & \text{if } \bar{y}_x \neq y_x, \bar{y}_x \in \mathbb{Z}^C \end{cases} \tag{3}$$

where $\bar{y}_x$ is one-hot encoded, and β is a parameter bounded in **Theorem 3** under a privacy budget ϵ_Y.

Randomizing the label y_x provides a complete LDP protection to each local training sample (e_x, y_x). All the perturbed training samples (e'_x, y'_x) are included in a local dataset D'_u, which will be used to train the model $f^\theta : \mathbb{R}^r \to \mathbb{R}^C$, i.e., $e'_x = \mathcal{E}(v'_x)$ where $\mathcal{E}(\cdot)$ is a decoding function, (Alg. 1, lines 20-22). The training will never access the original data D_u. All other operations remain the same with our aforementioned FL setting.

4 Privacy Guarantees of BitRand

In this section, we focus on bounding formal privacy loss of BitRand for input and label protection. To achieve our goal, we need to bound α and β in Eqs. 2 and 3 such that our algorithm preserves LDP for each training sample $(x, y_x) \in D_u$ given $(v'_x, y'_x) \in D'_u$. Note that the decoding $e'_x = \mathcal{E}(v'_x)$ does not incur any extra privacy risk following the post-processing property (Dwork & Roth, 2014). Given v_x and $\widetilde{v}_x$ can be different at any bit, for the LDP condition to hold, the ratio of two probabilities $\frac{P(f\text{-RR}(v_x)=v_z)}{P(f\text{-RR}(\widetilde{v}_x)=v_z)}$ needs to be bounded by $\exp(\epsilon_X)$ with $v_z \in Range(f\text{-RR})$.

Given a feature a, i.e., one of the r features, let us first consider a bit i in the encoding vector v_a. Intuitively, when we apply our f-RR only on the bit i in v_a (i.e., all the other bits remain the same), denoted as f-RR(v_a, i), the l_1-sensitivity of the bit i is 1. This is because, given *two neighboring vectors v_a and $v_{a|i}$ that differs only at the bit i*, we have that $\forall i \in v_a : \arg\max_{v_a} \|f\text{-RR}(v_a, i) - f\text{-RR}(v_{a|i}, i)\|_1 = 1$. However, the coordinating server can infer the decoded features $\mathcal{E}(f\text{-RR}(v_a))$ instead of just the intermediate result f-RR(v_a). Thus, we need to quantify the l_1-sensitivity of a single encoding bit $i \in v_a$ to determine just how accurately we can return the decoded features $\mathcal{E}(f\text{-RR}(v_a))$ through our randomization f-RR applied on v_a. Following (Dwork & Roth, 2014), the sensitivity Δ_i of a bit i can be quatified as follows:

Definition 2. *Bit l_1-sensitivity. Given two neighboring vectors v_a and $v_{a|i}$ that differs only at a bit i, the sensitivity Δ_i captures the magnitude by which the bit i can change the decoding function $\mathcal{E}(f\text{-}RR(\cdot))$ in the worst case, as follows:*

$$\forall i \in [0, rl-1] : \Delta_i = \max_{v_a} \|\mathcal{E}\big(f\text{-}RR(v_a)\big) - \mathcal{E}\big(f\text{-}RR(v_{a|i})\big)\|_1 \tag{4}$$

Based on Eq. 4, sensitivities Δ_i of all the bits in v_x are bounded in the following lemma.

Lemma 1. *The l_1-sensitivity of a single binary encoding bit is bounded as follows:*

$$\forall i \in [0, rl-1] : \Delta_i = \begin{cases} 2^{m+1}, & \textit{if } i \textit{ is a sign bit} \\ 2^{m-i\%l}, & \textit{if } i \textit{ is an integer/fraction bit} \end{cases} \tag{5}$$

All the proofs are in Appendix. Unlike existing RR mechanisms, we incorporate the l_1-sensitivity Δ_i into the privacy loss bound of f-RR by ensuring that the privacy loss in randomizing a bit i is bounded by the privacy loss in the embedded feature space. By doing so, we can derive tighter privacy loss bounds as discussed next.

Given Δ_i, there always exists a Laplace noise injected into the feature a, i.e., $\mathcal{M}(v_a, i) = \mathcal{E}(v_a) + Lap(\Delta_i/\epsilon_i)$, to achieve ϵ_i-LDP in the embedded feature space (Dwork & Roth, 2014). In other words, $\frac{P(\mathcal{M}(v_a,i)=z)}{P(\mathcal{M}(v_{a|i},i)=z)} \leq \exp(\frac{\epsilon_i|\mathcal{E}(v_a)-\mathcal{E}(v_{a|i})|}{\Delta_i})$ and $z \in Range(\mathcal{M})$. To ensure that the privacy loss in randomizing the bit i is bounded by the privacy loss in the embedded feature space is to find α in Eq. 2 such that: $\frac{P(f\text{-RR}(v_a,i)=v_z)}{P(f\text{-RR}(v_{a|i},i)=v_z)} \leq \exp(\frac{\epsilon_i|\mathcal{E}(v_a)-\mathcal{E}(v_{a|i})|}{\Delta_i})$. However, randomizing a binary encoding bit i given v_a and $v_{a|i}$ results in a smaller l_1-distance $|\mathcal{E}(f\text{-RR}(v_a,i))-\mathcal{E}(f\text{-RR}(v_{a|i},i))|$ compared with $|\mathcal{E}(v_a)-\mathcal{E}(v_{a|i})|$; since $|\mathcal{E}(f\text{-RR}(v_a,i))-\mathcal{E}(f\text{-RR}(v_{a|i},i))| \leq |\mathcal{E}(v_a)-\mathcal{E}(v_{a|i})|$. Thus, we can derive a tighter bound by replacing $|\mathcal{E}(v_a)-\mathcal{E}(v_{a|i})|$ with $|\mathcal{E}(f\text{-RR}(v_a,i))-\mathcal{E}(f\text{-RR}(v_{a|i},i))|$. Given $v_a(i)$ is the bit i in v_a, we have

$$\frac{P(f\text{-RR}(v_a,i)=v_z)}{P(f\text{-RR}(v_{a|i},i)=v_z)} = \frac{P(f\text{-RR}(v_a(i))=v_z(i))}{P(f\text{-RR}(v_{a|i}(i))=v_z(i))} \times \prod_{j\neq i, j\in[0,l-1]} \frac{P(v_a(j)=v_z(j))}{P(v_{a|i}(j)=v_z(j))}$$
$$= \frac{P(f\text{-RR}(v_a(i))=v_z(i))}{P(f\text{-RR}(v_{a|i}(i))=v_z(i))} \leq \exp(\frac{\epsilon_i|\mathcal{E}(f\text{-RR}(v_a,i))-\mathcal{E}(f\text{-RR}(v_{a|i},i))|}{\Delta_i}) \quad (6)$$

However, finding a closed-form solution of α for the tight privacy bound in Eq. 6 is non-trivial, since ϵ_i is intractable. To address this, we consider two cases: (1) $\frac{P(f\text{-RR}(v_a(i))=v_z(i))}{P(f\text{-RR}(v_{a|i}(i))=v_z(i))} \geq 1$ below, and (2) $0 < \frac{P(f\text{-RR}(v_a(i))=v_z(i))}{P(f\text{-RR}(v_{a|i}(i))=v_z(i))} < 1$ in Appendix D. Since Δ_i captures the magnitude by which the bit i can change the decoding function $\mathcal{E}(\cdot)$ in the worst case, we have $\frac{\Delta_i}{|\mathcal{E}(f\text{-RR}(v_a,i))-\mathcal{E}(f\text{-RR}(v_{a|i},i))|} \geq 1$. As a result, we have

$$\frac{P(f\text{-RR}(v_a(i))=v_z(i))}{P(f\text{-RR}(v_{a|i}(i))=v_z(i))} \leq \Big(\frac{P(f\text{-RR}(v_a(i))=v_z(i))}{P(f\text{-RR}(v_{a|i}(i))=v_z(i))}\Big)^{\frac{\Delta_i}{|\mathcal{E}(f\text{-RR}(v_a,i))-\mathcal{E}(f\text{-RR}(v_{a|i},i))|}} \leq \exp(\epsilon_i) \quad (7)$$

Eq. 7 enables us to quantify a *generalized privacy loss bound* of a RR mechanism, in which different bits have different sensitivities by randomizing all the bits in v_x independently in Theorem 1.

Theorem 1. *Generalized privacy loss bound. The privacy loss for randomizing a binary encoding vector v_x is bounded as follows:*

$$\frac{P(f\text{-}RR(v_x)=v_z)}{P(f\text{-}RR(\widetilde{v}_x)=v_z)} \leq \prod_{i=0}^{rl-1}\Big(\frac{P(f\text{-}RR(v_x(i))=v_z(i))}{P(f\text{-}RR(v_{x|i}(i))=v_z(i))}\Big)^{\frac{\Delta_i}{|\mathcal{E}(f\text{-}RR(v_x,i))-\mathcal{E}(f\text{-}RR(v_{x|i},i))|}} \leq \exp(\sum_{i=0}^{rl-1}\epsilon_i) \quad (8)$$

Now, we enforce the condition $\sum_{i=0}^{rl-1}\epsilon_i = \epsilon_X$ to ensure that the total privacy budget will be bounded by ϵ_X. Based upon that, we derive a closed-form solution showing that there always exists an upper bound of α so that v'_x preserves ϵ_X-LDP given v_x in **Theorem 2** (Alg. 1, line 17).

Theorem 2. $\forall\alpha : 0 < \alpha \leq \sqrt{\frac{\epsilon_X+rl}{2r\sum_{i=0}^{l-1}\exp(2\frac{\epsilon_X}{l}i\%l)}}$, *the f-RR mechanism satisfies ϵ_X-LDP: $\frac{P(f\text{-}RR(v_x)=z)}{P(f\text{-}RR(\widetilde{v}_x)=z)} < \epsilon_X$, where v_x and $\widetilde{v}_x$ can be different at any bit, and $z \in Range(f\text{-}RR)$.*

Regarding to the ground-truth label y_x, given a privacy budget ϵ_Y, we show that there always exists an upper bound of β so that y'_x preserves ϵ_Y-LDP given y_x.

Theorem 3. $\forall\beta : \beta \leq \epsilon_Y - \ln(C-1)$, *the label-RR mechanism (Alg. 1, line 18) satisfies ϵ_Y-LDP: $\frac{P(label\text{-}RR(y_x)=z|y_x)}{P(label\text{-}RR(\widetilde{y}_x)=z|\widetilde{y}_x)} \leq \exp(\epsilon_Y)$, given any distinct labels y_x and $\widetilde{y}_x$, and $z \in Range(label\text{-}RR)$.*

From Theorems 2 and 3, our BitRand preserves ϵ_X-LDP for the vector v_x and ϵ_Y-LDP for label y_x. The gradients $\bigtriangledown^u_{\theta_t}$ preserve (ϵ_X, ϵ_Y)-LDP in any training rounds t for any training samples $(x, y_x) \in D_u$ and for all clients $u \in [1, N]$; since, $\forall u, t$: $\bigtriangledown^u_{\theta_t}$ are computed from the randomized training samples $\{(v'_x, y'_x)\}_{n_u}$ without accessing any further information from $\{(x, y_x)\}_{n_u}$.

5 Privacy and Utility Trade-off

As shown in Theorem 1, we can derive a tighter privacy loss bound. Therefore, we focus on understanding how BitRand can address the privacy-utility trade-off in comparison with existing approaches by theoretically studying: **(1)** the utility of f-RR regarding the expected error bound (**Theorem 4**), and **(2)** the trade-off between privacy budget and randomization probabilities. *All statistical tests are 2-tail t-tests.*

Expected Error Bounds. We analyze the data utility through *expected error*, denoted as ξ_a, measuring the

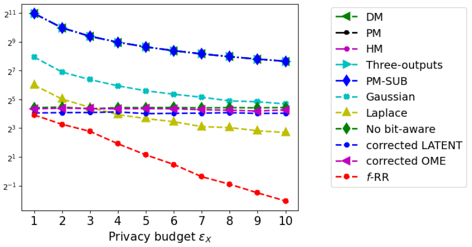

Figure 3: Expected error bound comparison for an embedded feature a with $r = 1,000$, $l = 10$, and $m = 5$.

expected change of each embedded feature a after applying f-RR: $\xi_a = \mathbb{E}|\mathcal{E}(f\text{-RR}(v_a)) - \mathcal{E}(v_a)|$. The *smaller expected error* is, the *better data utility* the randomization mechanism achieves. The expected error ξ_a is bounded by $\sum_{i\in[0,l-1]} q_{Xi} \times \Delta_i$.

Theorem 4. *The f-RR expected error bound is quantified by* $\xi_a = \mathbb{E}|\mathcal{E}(f\text{-}RR(v_a)) - \mathcal{E}(v_a)| = \sum_{i\in[0,l-1]} q_{Xi} \times \Delta_i$.

Theorem 4 can be directly applied to quantify the expected error bounds of f-RR without the bit-aware term $i\%l/l$, corrected LATENT (Appendix I), and corrected OME (Appendix J). Regarding existing mechanisms applied on the embedded feature a, including Duchi mechanism (DM) (Duchi et al., 2013), Piecewise mechanism (PM) (Wang et al., 2019a), Hybrid mechanism (HM) (Wang et al., 2019a), Suboptimal mechanism (PM-SUB) (Zhao et al., 2020b), Gaussian and Laplace (Dwork & Roth, 2014), we derive a general form of expected error bounds ξ_a for these mechanisms as: $\xi_a = \mathbb{E}|\mathcal{M}(a) - a| \approxeq 1/r \sum_{a\in[1,r]} |\mathcal{M}(a) - a|$ where $\mathcal{M}$ is an ϵ_X-LDP preserving mechanism, since $\lim_{r\to\infty} \mathbb{E}|\mathcal{M}(a) - a| = 1/r \sum_{a\in[1,r]} |\mathcal{M}(a) - a|$.

Figure 3 illustrates the expected error bound of each algorithm as a function of ϵ_X. It is obvious that f-RR has significantly tighter expected error bounds compared with baseline approaches under a wide range of privacy budgets given reasonable large numbers of embedded features and encoding bits ($p = 0.02$); thus indicating that our mechanism achieves better data utility compared with the baselines. The improvement of our f-RR over existing mechanisms is larger when ϵ_X increases.

To profoundly study the data utility, we take a depth look into bit-level analysis by relaxing Theorem 4 into **(1)** an expected error bound $\xi_i = q_{Xi} \times \Delta_i$ for each bit $i \in [0, l-1]$, and **(2)** an average top-k expected error bound $\xi_{top-k} = 1/k \sum_{i=0}^{k} \xi_i, \forall k \in [0, l-1]$. Figure 11 (Appendix K) show that, at the bit-level, f-RR achieves smaller values of ξ_i for most important bits, especially the sign bit and integer bits, and comparable ξ_i for least important bits, i.e., fraction bits. The gap between f-RR and the baselines are significantly larger given the ξ_{top-k}. We obtain smaller values of ξ_{top-k} for all $k \in [0, l-1]$, under a tight privacy budget $\epsilon_X = 0.1$. Importantly, when increasing privacy budget ϵ_X (Figures 11b,c), the gap between f-RR and the baselines is larger. In fact, the expected error bounds in f-RR is reduced while the expected error bounds in the baselines are remained the same.

Privacy budget and randomization probabilities trade-off. Compared with existing RR mechanisms (Lyu et al., 2020a; Arachchige et al., 2019; Sun et al., 2021; Zhao et al., 2020b; Duchi & Rogers, 2019; Wang et al., 2019a; Liu et al., 2020), in our algorithm, bits with a *stronger influence* on the model utility, e.g., sign bits and integer bits, have *smaller randomization probabilities* q_X, and vice-versa. This is because we consider the influence of each bit i through the term $\frac{i\%l}{l}$ in modeling the randomization probabilities q_X (and p_X). This unique property of our algorithm enables us to better optimize the trade-off between privacy loss and model utility.

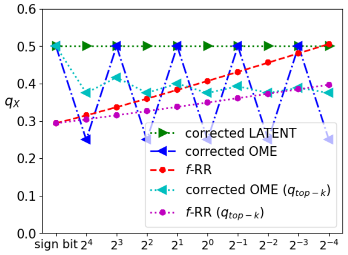

Figure 4: Randomization probability q_X and $q_{top\text{-}k}$, given $l = 10$, $r = 1,000$, and $\epsilon_X = 1$.

To demonstrate this, we examine the behavior of q_X across binary encoding bits under a wide range of $\epsilon_X \in \{0.1, 1, 2\}$, given reasonable values of r and l, i.e., $r = 1,000$ and $l = 10$ (Figures 4 and 12, Appendix K). Our mechanism achieves a smaller randomization probability q_X than the corrected LATENT in all cases ($p = 3.7e-9$), especially more significant bits, such as sign bits and integer bits. The gap is more prominent when ϵ_X increases. This observation is less obvious when comparing our mechanism with the corrected OME, given an uneven randomization probability q_X across bits in the corrected OME. To better show the comparison, we draw an average top-k measure curve: $\forall k \in [0, l-1] : q_{top\text{-}k} = 1/k \sum_{i=0}^{k} q_i$, where q_i is the bit i's q_X, to evaluate the average q_X across bits. The smaller $q_{top\text{-}k}$ is, the better the randomization probability q_X is. Given a tight privacy budget $\epsilon_X = 0.1$, our mechanism and the corrected OME have a similar $q_{top\text{-}k}$. However, when ϵ_X increases, i.e., $\epsilon_X \in \{1, 2\}$, our mechanism achieves significantly smaller values of $q_{top\text{-}k}$ than the corrected OME ($p = 5.1e-3$).

6 Dimension-Elastic Analysis

In existing RR mechanisms, the curse of privacy composition is rooted in the privacy composition across bits l and features r (Duchi et al., 2013; Lyu et al., 2020a; Arachchige et al., 2019), gradients $\bigtriangledown^u_{\theta_t}$ (Zhao et al., 2020b; Wang et al., 2019a), and training rounds T (Zhao et al., 2020b; Wang et al., 2019a). Thus, increasing the dimensions of l, r, $\bigtriangledown^u_{\theta_t}$, and T either significantly increases the privacy budget (i.e., resulting in loose privacy protection) (Wang et al., 2019a; 2017) or notably affects the randomization probabilities (i.e., the value transmitted correctly through the randomization becomes smaller resulting in poor utility (Wang et al., 2016a)) (Lyu et al., 2020a; Arachchige et al., 2019).

In Theorem 1, the privacy composition across bits and features is unavoidable. However, the values of embedded features transmitted correctly through our randomization mechanism is minimally affected when increasing the dimensions of r, l, $\bigtriangledown^u_{\theta_t}$, T, and C under the same ϵ_X and ϵ_Y. That enable us to evade the curse of privacy composition when working with complex models and tasks under rigorous LDP protection. To shed light into this property, we conduct a theoretical analysis to examine: **(1)** How the dimensions of r, l, gradients $\bigtriangledown^u_{\theta_t}$, and training rounds T impact the privacy budget ϵ_X and the randomization probabilities q_X and p_X $(= 1 - q_X)$; and **(2)** How the number of model outcomes C impacts the privacy budget ϵ_Y and the randomization probabilities q_Y and p_Y. We select the upper bounds of $\alpha = \sqrt{(\epsilon_X + rl)/(2r\sum_{i=0}^{l-1}\exp(2\epsilon_X\frac{i}{l}))}$ and $\beta = \epsilon_Y - \ln(C-1)$ (Theorems 2, 3) in our analysis.

Dimensions of gradients $\bigtriangledown^u_{\theta_t}$ and training rounds T. In BitRand, the clients only use the perturbed samples (v'_x, y'_x) to train their local models without accessing any further information from (x, y_x). Thus, the privacy budgets ϵ_X and ϵ_Y are independent of the dimension of gradients $\bigtriangledown^u_{\theta_t}$ and the training rounds T, i.e., following the post-processing property in DP (Dwork & Roth, 2014). Also, the size of $\bigtriangledown^u_{\theta_t}$ and T do not affect the randomization probabilities, since $\bigtriangledown^u_{\theta_t}$ and T are not used to model q_X, p_X, q_Y, and p_Y as in Eqs. 2 and 3.

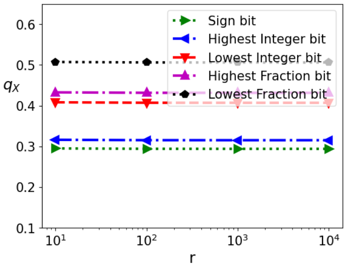

Figure 5: Randomization probability q_X as a function of r with fixed $l = 10$ and $\epsilon_X = 1$.

Dimensions of embedded features r and encoding bits l. Varying the dimensions of r and l does not affect the privacy budget $\epsilon_X \in \mathbb{R}^+$, since there always exists an α for Theorem 2 to hold. However, it is necessary to understand the influence of varying r and l on the privacy-utility trade-off. We theoretically analyze the impacts of r and l on the randomization probabilities q_X and p_X, given fixed values of ϵ_X. A model is expected to achieve higher model utility given smaller values of q_X (higher values of p_X) under the same privacy budget. We examine q_X and p_X in the following experiments: **(i)** Fixing l, then varying r; and **(ii)** Fixing r, then varying l.

Figures 5 and 13 (Appendix K) illustrate q_X as a function of r, under $l \in \{5, 20, 100, 1,000\}$ and $\epsilon_X \in \{0.1, 1, 2\}$. Varying r does not affect the randomization probability q_X (and p_X) for all the bits in v_x. To explain this, we take a deeper look into the α's bound, which is the only factor affecting q_X and p_X. Given fixed ϵ_X and l, $\sum_{i=0}^{l-1}\exp(2\epsilon_X\frac{i}{l})$ is a constant, denoted $\mathcal{C}$. So, we have $\alpha = \sqrt{(\epsilon_X + rl)/(2r\mathcal{C})} = \sqrt{(\frac{\epsilon_X}{r} + l)/(2\mathcal{C})} \approxeq \sqrt{l/(2\mathcal{C})}$, since $\frac{\epsilon_X}{r} \approxeq 0.0$ in practice. Thus, with fixed ϵ_X and l, q_X and p_X are r-elastic, given α approximately is a constant $\sqrt{l/(2\mathcal{C})}$.

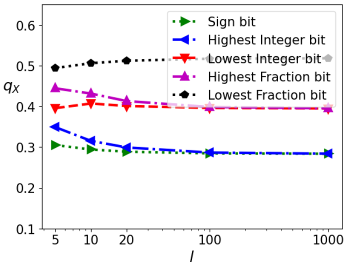

Figure 6: Randomization probability q_X as a function of l with fixed $r = 1,000$ and $\epsilon_X = 1$.

Now, we fix $r = 1,000$, which is a decent number of embedded features, and show q_X as a function of l under a wide range of $r \in [10, 10,000]$ and $\epsilon_X \in \{0.1, 1, 2\}$ (Figures 6 and 14, Appendix K). Given a tight privacy budget $\epsilon_X = 0.1$, varying l does not affect the randomization probability q_X, i.e., $m = \lfloor l/2 \rfloor$ in our analysis covering most values of embedded features in practice. However, with higher values of $\epsilon_X \in \{1.0, 2.0\}$, using more encoding bits l lowers q_X for most important bits, i.e., sign and integer bits; while increasing q_X for least important bits, i.e., fraction bits. When l is large enough ($l \geq 20$), the randomization probability q_X is l-elastic since the impact of l becomes marginal to all the bits. This is also true for p_X.

Number of model outcomes C. Similar to ϵ_X, from Eq. 3 and Theorem 3, the privacy budget ϵ_Y is not directly affected by the number of model outcomes C, since $\forall C, \epsilon_X$: $\exists\beta$ for Theorem 3 to hold. However, C may impact the trade-off between privacy and model utility by affecting the randomization probabilities q_Y and p_Y. Figure 7 shows that, when C is sufficiently large, i.e., $C \geq 100$, the randomization probability q_Y is C-elastic since the impact of C on q_Y is marginal given a wide range of the privacy budget ϵ_Y. This is also true for p_Y. When ϵ_Y increases, the randomization probability q_Y becomes smaller (p_Y becomes larger). This is a reasonable observation.

Thanks to the bit-aware and dimension-elastic properties, our BitRand can achieve high data utility, especially under tight privacy budgets and expected error bounds.

7 Experimental Results

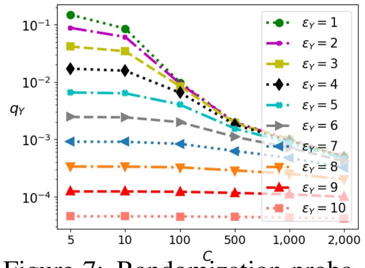

Figure 7: Randomization probability q_Y with varying ϵ_Y and C.

We have conducted an extensive experiment on benchmark datasets under two fundamental FL tasks, text and image classification, to shed light on understanding 1) the interplay among privacy budget and model utility in BitRand, 2) the effectiveness of the dimension-elastic and bit-aware properties on model utility, and 3) different settings of applying RR to preserve LDP.

Baseline Approaches. We consider a variety of LDP-preserving mechanisms as baseline approaches: **(1)** Binary encoding approaches, including the **corrected LATENT** (Arachchige et al., 2019) and the **corrected OME** (Lyu et al., 2020a) (Appendices I and J); **(2) LDP-FL** (Sun et al., 2021); **(3)** Duchi mechanism (**DM**) (Duchi et al., 2013); **(4)** Piecewise mechanism (**PM**) (Wang et al., 2019a); **(5)** Hybrid mechanism (**HM**) (Wang et al., 2019a); **(6) Three-Outputs** mechanism (Zhao et al., 2020b); **(7)** Suboptimal mechanism (**PM-SUB**) (Zhao et al., 2020b); and **(8) Label-Laplace** (Phan et al., 2020). Each baseline approach is applied to randomize (when applicable): **(i)** Embedded features e_x; **(ii)** Gradients $\bigtriangledown^u_{\theta_t}$; and **(iii)** Gradients $\bigtriangledown^u_{\theta_t}$ with a recent anonymizer (Sun et al., 2021) to reduce the privacy budget consumption. In addition, Label-Laplace is used as a baseline to protect the ground-truth labels y_x. Note that, in our experiment, we use the upper bound of β resulting in the same randomizing probabilities as in LabelDP. Therefore, we do not include LabelDP in comparison. More details about the difference of $label$-RR and LabelDP are in Appendix G. These settings are widely accepted to preserve LDP in FL; thus, offering a comprehensive view of preserving LDP in FL. Note that LATENT, OME, and BitRand can only be applied on embedded features e_x; while LDP-FL can only be applied on gradients $\bigtriangledown^u_{\theta_t}$ with and without the anonymizer (Sun et al., 2021). We include the **Noiseless** FL model trained on the original data D_u to show upper-bounds and a **Random** guess model to understanding model utility better.

Datasets, Metrics, and Model Configuration. The complete details of the datasets, metrics, and model configuration are in Appendix L. We carried out our experiments on two textual datasets and two image datasets, including the AG dataset (Gulli et al., 2012), our collected Security and Exchange Commission (SEC) financial contract dataset, the large-scale celebFaces attributes (CelebA) dataset (Liu et al., 2015), and the Federated Extended MNIST (FEMNIST) dataset (Caldas et al., 2018). We use the test accuracy and the test area under the curve (AUC) as evaluation metrics. Models with higher values of test accuracy and AUC are better. We use the BERT-Base (Uncased) pre-trained model (ber; Devlin et al., 2018) to extract embedded features in the AG and SEC datasets. In the CelebA and FEMNIST datasets, we use the ResNet-18 pre-trained model (img; He et al., 2016). For text and image classification tasks, we use two fully connected layers on top of embedded features, each of which consists of $1,500$ hidden neurons and uses a ReLU activation function.

Evaluation Results. Comprehensive results show that BitRand offers stronger privacy protection with higher model utility, compared with all baseline approaches, as discussed next.

LDP-preserving approaches applied on the embedded features e_x. Baseline approaches do not work well when they are applied on embedded features e_x (Figures 15 and 19, Table 3, Appendix L). In SEC, AG, and FEMNIST datasets, BitRand achieves the highest model utility compared with the best baseline approach, which is the corrected OME, under a tight privacy budget $\epsilon_X = 1$. In terms of accuracy and AUC values, BitRand ($\epsilon_Y = \infty$) achieves an improvement of 46.03% and 38.51% in the AG dataset ($p = 2.7e - 22$), 13.69% and 13.79% in the SEC dataset ($p = 4.1e - 12$), and 21.62% and 13.42% in the FEMNIST dataset ($p = 5.6e - 11$) respectively. In the CelebA dataset (Table 3, Appendix L), BitRand outperforms the best baseline approach, i.e., PM-SUB, with an average improvement of 1.66% across all 40 attributes in terms of AUC measure ($p = 1.2e - 2$). Since the CelebA dataset is highly imbalanced, we use the AUC measure instead of the model accuracy. The gaps between BitRand and the baseline approaches are significantly wider when the privacy budget ϵ_X is larger. In addition to $\epsilon_X = 1$, with a tight privacy budget for the class labels $\epsilon_Y \in \{1, 2.5\}$, BitRand still outperforms baseline approaches in most of cases, offering stronger privacy protection with better model utility, i.e., LDP at both embedded feature and label levels instead of only LDP on the embedded features as in baseline approaches.

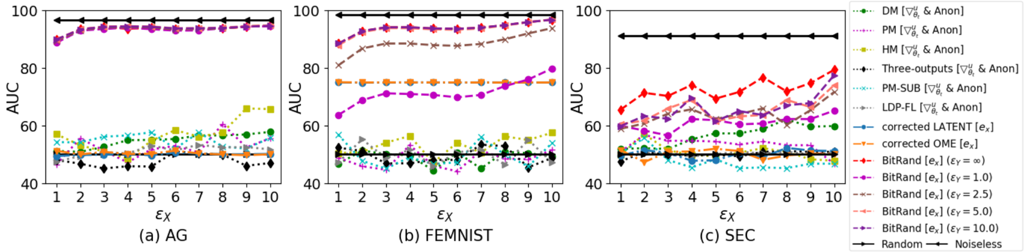

Figure 8: AUC values of each algorithm applied on the gradients $\bigtriangledown^u_{\theta_t}$ with the anonymizer.

The key reason is that, in the baseline approaches, the model utility is significantly affected by the size of the embedded features. Thanks to the dimension-elastic and bit-aware properties, BitRand can achieve high model accuracy and AUC values, especially under tight privacy budgets. In addition, BitRand achieves the highest improvement in the AG dataset, since it is a balanced dataset compared with the highly imbalanced CelebA dataset, in which BitRand achieves the least improvement. Addressing imbalanced data in FL under DP (Huang et al., 2020) is out-of-scope of our study.

LDP-preserving approaches applied on on gradients $\bigtriangledown^u_{\theta_t}$ without and with the anonymizer (Sun et al., 2021). We observe the same phenomenon when baseline approaches are applied on gradients $\bigtriangledown^u_{\theta_t}$ without and with the anonymizer (Sun et al., 2021), even though the gaps between BitRand and baseline approaches are (marginally) smaller (Figures 8, 16-17, 20, and Tables 4, 5, Appendix L). Without using the anonymizer in the baseline approaches, in terms of accuracy and AUC, compared with the best baseline approach PM-SUB, BitRand ($\epsilon_X = 1$, $\epsilon_Y = 1$) achieves an improvement of 44.95% and 37.52% in the AG dataset ($p = 3.9e - 20$), 12.82% and 12.92% in the SEC dataset ($p = 1.3e - 11$), 24.17% and 13.40% in the FEMNIST dataset ($p = 4.1e - 11$). When the anonymizer is applied in the baseline approaches, in terms of accuracy and AUC, compared with the best baseline approache HM, our BitRand achieves an improvement of 39.38% and 32.75% in the AG dataset ($p = 1.2e - 16$), 13.59% and 13.69% in the SEC dataset ($p = 2.1e - 10$), and 23.12% and 37.02% in the FEMNIST dataset ($p = 2.8e - 11$). Regarding the CelebA dataset, BitRand outperforms the best baseline approaches, which are Three-outputs and HM, with improvements of 1.28% and 0.3%, in the cases of with and without the anonymizer, across all 40 attributes in terms of AUC ($p = 3.1e-2$). The model utility in baselines is affected by the size of gradients and the training rounds (when the anonymizer is not applied) and their finite numbers of randomization outputs of the gradients (Zhao et al., 2020b). Thanks to the bit-aware and dimension-agnostic properties, BitRand can achieve high model utility under rigorous LDP protection.

LDP-preserving labels. Figures 18, 21, and Table 3 (Appendix L) present the model utility of BitRand as a function of the privacy budgets ϵ_X and ϵ_Y, in which $label$-RR is replaced by the Label-Laplace, denoted as f-RR & Label-Laplace. $label$-RR outperforms the Label-Laplace in all values of ϵ_X, ϵ_Y, and datasets. Under rigorous LDP protection $\epsilon_Y = 1$ given $\epsilon_X \in [1, 10]$, there is an average improvement of 9.65% accuracy and 7.92% AUC in the AG dataset ($7.3e - 6$), 7.84% accuracy and 7.35% AUC in the SEC dataset ($1.2e - 5$), and 9.91% accuracy and 10.55% AUC in the FEMNIST dataset ($p = 9.8e - 5$), and 2.04% AUC in the CelebA dataset ($p = 1.6e - 2$). The gaps are delicately smaller in the AG and SEC datasets, and substantially larger in the FEMNIST and CelebA datasets when ϵ_Y is increased. Given $\epsilon_Y = 2.5$, there is an average improvement of 1.71% accuracy and 1.37% AUC in the AG dataset ($8.5e - 2$), 4.65% accuracy and 4.73% AUC in the SEC dataset ($6.9e - 3$), and 14.43% accuracy and 12.02% AUC in the FEMNIST dataset ($p = 1.9e - 4$), and 4.24% AUC in the CelebA dataset ($p = 2.3e - 2$). The reason is that Label-Laplace injects Laplace noise across C classes in a label y_x causing more noisy model outcomes compared with $label$-RR, in which only one of the C model outcomes is selected as the result of the randomization.

8 Conclusion

In this paper, we introduced a bit-aware algorithm, called BitRand, providing rigorous LDP protection to both embedded features and labels in FL via binary encoding. In BitRand, the trade-off between the privacy budget consumption and randomization probabilities is dimension-elastic to the numbers of embedded features, encoding bits, gradients, model outcomes, and training rounds, enabling us to work with complex models and FL tasks. We further optimize the randomization probabilities by having smaller randomization probabilities assigned to more critical bits and vice-versa under the same privacy budgets. Theoretical analysis and extensive experiments showed that our BitRand outperforms baseline approaches in text and image classification.

References

Cometomyhead academic news search engine. http://newsengine.di.unipi.it.

Google ai. pre-trained bert model. https://bert-as-service.readthedocs.io/en/latest/section/get-start.html#installation.

Pre-trained resnet-18 model. https://github.com/christiansafka/img2vec.

Induction proofs. https://www.purplemath.com/modules/inductn3.htm.

M. Abadi, A. Chu, I. Goodfellow, H. B. McMahan, I. Mironov, K. Talwar, and L. Zhang. Deep learning with differential privacy. In *ACM SIGSAC Conference on Computer and Communications Security*, pp. 308–318, 2016.

J. Acharya, Z. Sun, and H. Zhang. Hadamard response: Estimating distributions privately, efficiently, and with little communication. In *The 22nd International Conference on Artificial Intelligence and Statistics*, pp. 1120–1129, 2019.

M. Alvim, K. Chatzikokolakis, C. Palamidessi, and A. Pazii. Local differential privacy on metric spaces: optimizing the trade-off with utility. In *2018 IEEE 31st Computer Security Foundations Symposium*, pp. 262–267, 2018.

P. C. M. Arachchige, P. Bertok, I. Khalil, D. Liu, S. Camtepe, and M. Atiquzzaman. Local differential privacy for deep learning. *IEEE Internet of Things Journal*, 7(7):5827–5842, 2019.

B. Balle, J. Bell, A. Gascón, and K. Nissim. The privacy blanket of the shuffle model. In *Annual International Cryptology Conference*, pp. 638–667, 2019.

R. Bassily and A. Smith. Local, private, efficient protocols for succinct histograms. In *ACM Symposium on Theory of Computing*, pp. 127–135, 2015.

R. Bassily, K. Nissim, U. Stemmer, and A. Thakurta. Practical locally private heavy hitters. *arXiv preprint arXiv:1707.04982*, 2017.

Abhishek Bhowmick, John Duchi, Julien Freudiger, Gaurav Kapoor, and Ryan Rogers. Protection against reconstruction and its applications in private federated learning. *arXiv preprint arXiv:1812.00984*, 2018.

Robert Istvan Busa-Fekete, Umar Syed, Sergei Vassilvitskii, et al. On the pitfalls of label differential privacy. In *NeurIPS 2021 Workshop LatinX in AI*, 2021.

S. Caldas, S. M. K. Duddu, P. Wu, T. Li, J. Konečnỳ, H. B. McMahan, V. Smith, and A. Talwalkar. Leaf: A benchmark for federated settings. *arXiv preprint:1812.01097*, 2018.

N. Carlini, F. Tramer, E. Wallace, M. Jagielski, A. Herbert-Voss, K. Lee, A. Roberts, T. Brown, D. Song, U. Erlingsson, et al. Extracting training data from large language models. *arXiv preprint arXiv:2012.07805*, 2020.

A. Cheu, A. Smith, J. Ullman, D. Zeber, and M. Zhilyaev. Distributed differential privacy via shuffling. In *EUROCRYPT*, pp. 375–403, 2019.

G. Cohen, S. Afshar, J. Tapson, and A. Van Schaik. EMNIST: Extending MNIST to handwritten letters. In *International Joint Conference on Neural Networks*, pp. 2921–2926, 2017.

G. Cormode, T. Kulkarni, and D. Srivastava. Marginal release under local differential privacy. In *ACM SIGMOD*, pp. 131–146, 2018.

J. Devlin, M. W. Chang, K. Lee, and K. Toutanova. Bert: Pre-training of deep bidirectional transformers for language understanding. *arXiv preprint arXiv:1810.04805*, 2018.

J. Dong, A. Roth, and W. J. Su. Gaussian differential privacy. *arXiv preprint arXiv:1905.02383*, 2019.

J. Duchi and R.n Rogers. Lower bounds for locally private estimation via communication complexity. In *COLT*, pp. 1161–1191, 2019.

J. C. Duchi, M. I. Jordan, and M. J. Wainwright. Local privacy and statistical minimax rates. In *IEEE Protocols for secure computations*, pp. 429–438, 2013.

J. C. Duchi, M. I. Jordan, and M. J. Wainwright. Minimax optimal procedures for locally private estimation. *Journal of the American Statistical Association*, 113(521):182–201, 2018.

C. Dwork and A. Roth. The algorithmic foundations of differential privacy. *Found. Trends Theor. Comput. Sci.*, 9(3&#8211;4):211–407, 2014. ISSN 1551-305X.

U. Erlingsson, V. Pihur, and A. Korolova. Rappor: Randomized aggregatable privacy-preserving ordinal response. In *Proceedings of the 2014 ACM SIGSAC CCS*, pp. 1054–1067, 2014.

Ú. Erlingsson, V. Feldman, I. Mironov, A. Raghunathan, K. Talwar, and A. Thakurta. Amplification by shuffling: From local to central differential privacy via anonymity. In *ACM-SIAM SODA*, pp. 2468–2479, 2019.

G. Fanti, V. Pihur, and Ú. Erlingsson. Building a rappor with the unknown: Privacy-preserving learning of associations and data dictionaries. *arXiv preprint arXiv:1503.01214*, 2015.

M. Fredrikson, S. Jha, and T. Ristenpart. Model inversion attacks that exploit confidence information and basic countermeasures. In *ACM SIGSAC CCS*, pp. 1322–1333, 2015.

GDPR. The european data protection regulation. `https://gdpr-info.eu/`, 2018.

R. C. Geyer, T. Klein, and M. Nabi. Differentially private federated learning: A client level perspective. *arXiv preprint arXiv:1712.07557*, 2017.

B. Ghazi, N. Golowich, R. Kumar, P. Manurangsi, and C. Zhang. On deep learning with label differential privacy. *arXiv preprint arXiv:2102.06062*, 2021.

M. E. Gursoy, A. Tamersoy, S. Truex, W. Wei, and L. Liu. Secure and utility-aware data collection with condensed local differential privacy. *IEEE Transactions on Dependable and Secure Computing*, 2019.

A. Haeberlen, B. C. Pierce, and A. Narayan. Differential privacy under fire. In *USENIX Security Symposium*, volume 33, 2011.

K. He, X. Zhang, S. Ren, and J. Sun. Deep residual learning for image recognition. In *IEEE Conference on Computer Vision and Pattern Recognition*, pp. 770–778, 2016.

X. Huang, Y. Ding, Z. L. Jiang, S. Qi, X. Wang, and Q. Liao. DP-FL: a novel differentially private federated learning framework for the unbalanced data. *World Wide Web*, 23(4):2529–2545, 2020.

P. Kairouz, H. B. McMahan, B. Avent, A. Bellet, M. Bennis, A. N. Bhagoji, K. Bonawitz, Z. Charles, G. Cormode, R. Cummings, et al. Advances and open problems in federated learning. *arXiv preprint arXiv:1912.04977*, 2019.

S. Kim, H. Shin, C. Baek, S. Kim, and J. Shin. Learning new words from keystroke data with local differential privacy. *IEEE TKDE*, pp. 479–491, 2018.

Ruixuan L., Yang C., Hong C., Ruoyang G., and Masatoshi Y. FLAME: differentially private federated learning in the shuffle model. *CoRR*, abs/2009.08063, 2020.

R. Liu, Y. Cao, M. Yoshikawa, and H. Chen. Fedsel: Federated sgd under local differential privacy with top-k dimension selection. In *International Conference on Database Systems for Advanced Applications*, pp. 485–501, 2020.

Z. Liu, P. Luo, X. Wang, and X. Tang. Deep learning face attributes in the wild. In *ICCV*, December 2015.

L. Lyu, Y. Li, X. He, and T. Xiao. Towards differentially private text representations. In *Proceedings of the 43rd International ACM SIGIR Conference on Research and Development in Information Retrieval*, pp. 1813–1816, 2020a.

L. Lyu, H. Yu, and Q. Yang. Threats to federated learning: A survey. *arXiv preprint arXiv:2003.02133*, 2020b.

M. Malekzadeh, B. Hasircioglu, N. Mital, K. Katarya, M. E. Ozfatura, and D. Gündüz. Dopamine: Differentially private federated learning on medical data. *arXiv preprint arXiv:2101.11693*, 2021.

B. McMahan, E. Moore, D. Ramage, S. Hampson, and B. A. y Arcas. Communication-efficient learning of deep networks from decentralized data. In *Artificial Intelligence and Statistics*, pp. 1273–1282, 2017.

Ilya Mironov. On significance of the least significant bits for differential privacy. In *Proceedings of the 2012 ACM conference on Computer and communications security*, pp. 650–661, 2012.

N. H. Phan, M. T. Thai, H. Hu, R. Jin, T. Sun, and D. Dou. Scalable differential privacy with certified robustness in adversarial learning. In *ICML*, pp. 7683–7694, 2020.

Protection Regulation. General data protection regulation. *Intouch*, 2018.

X. Ren, C. M. Yu, W. Yu, S. Yang, X. Yang, J. A. McCann, and S. Y. Philip. Lopub: High-dimensional crowdsourced data publication with local differential privacy. *IEEE Transactions on Information Forensics and Security*, 13(9):2151–2166, 2018.

H. Shin, S. Kim, J. Shin, and X. Xiao. Privacy enhanced matrix factorization for recommendation with local differential privacy. *IEEE Transactions on Knowledge and Data Engineering*, 30(9): 1770–1782, 2018.

C. Song and A. Raghunathan. Information leakage in embedding models. In *ACM SIGSAC CCS*, pp. 377–390, 2020.

L. Sun, J. Qian, and X. Chen. LDP-FL: Practical private aggregation in federated learning with local differential privacy. *IJCAI*, 2021.

Cybersecurity Law. Cybersecurity law of the people's republic of china. `https://en.wikipedia.org/wiki/Cybersecurity_Law_of_the_People%27s_Republic_of_China`, 2016.

Gulli et al. Ag's corpus of news articles. `http://groups.di.unipi.it/~gulli/AG_corpus_of_news_articles.html`, 2012.

S. Truex, N. Baracaldo, A. Anwar, T. Steinke, H. Ludwig, R. Zhang, and Y. Zhou. A hybrid approach to privacy-preserving federated learning. In *Proceedings of the 12th ACM Workshop on Artificial Intelligence and Security*, pp. 1–11, 2019.

S. Wagh, X. He, A. Machanavajjhala, and P. Mittal. Dp-cryptography: marrying differential privacy and cryptography in emerging applications. *Communications of the ACM*, 64(2):84–93, 2021.

D. Wang and J. Xu. On sparse linear regression in the local differential privacy model. In *ICML*, pp. 6628–6637, 2019.

N. Wang, X. Xiao, Y. Yang, J. Zhao, S. C. Hui, H. Shin, J. Shin, and G. Yu. Collecting and analyzing multidimensional data with local differential privacy. In *IEEE ICDE*, pp. 638–649, 2019a.

S. Wang, L. Huang, P. Wang, H. Deng, H. Xu, and W. Yang. Private weighted histogram aggregation in crowdsourcing. In *International Conference on Wireless Algorithms, Systems, and Applications*, pp. 250–261, 2016a.

S. Wang, L. Huang, P. Wang, Y. Nie, H. Xu, W. Yang, X. Li, and C. Qiao. Mutual information optimally local private discrete distribution estimation. *arXiv preprint:1607.08025*, 2016b.

T. Wang, J. Blocki, N. Li, and S. Jha. Locally differentially private protocols for frequency estimation. In *26th USENIX Security Symposium*, pp. 729–745, 2017.

T. Wang, B. Ding, M. Xu, Z. Huang, C. Hong, J. Zhou, N. Li, and S. Jha. Improving utility and security of the shuffler-based differential privacy. *arXiv preprint arXiv:1908.11515*, 2019b.

T. Wang, B. Ding, M. Xu, et al. Murs: practical and robust privacy amplification with multi-party differential privacy. In *ACSAC*, 2019c.

S. L. Warner. Randomized response: A survey technique for eliminating evasive answer bias. *Journal of the American Statistical Association*, 60(309):63–69, 1965.

X. Xiong, S. Liu, D. Li, J. Wang, and X. Niu. Locally differentially private continuous location sharing with randomized response. *International Journal of Distributed Sensor Networks*, 15(8): 1550147719870379, 2019.

C. Xu, J. Ren, L. She, Y. Zhang, Z. Qin, and K. Ren. Edgesanitizer: Locally differentially private deep inference at the edge for mobile data analytics. *IEEE Internet of Things Journal*, 6(3):5140–5151, 2019.

Hongxu Y., Arun M., Arash V., Jose M. A., Jan K., and Pavlo M. See through gradients: Image batch recovery via gradinversion, 2021.

Q. Yang, Y. Liu, T. Chen, and Y. Tong. Federated machine learning: Concept and applications. *ACM Transactions on Intelligent Systems and Technology*, 10(2):1–19, 2019.

B. Zhao, K. R. Mopuri, and H. Bilen. idlg: Improved deep leakage from gradients. *arXiv preprint arXiv:2001.02610*, 2020a.

X. Zhao, Y. Li, Y. Yuan, X. Bi, and G. Wang. Ldpart: effective location-record data publication via local differential privacy. *IEEE Access*, 2019.

Y. Zhao, J. Zhao, M. Yang, T. Wang, N. Wang, L. Lyu, D. Niyato, and K. Y. Lam. Local differential privacy based federated learning for internet of things. *IEEE Internet of Things Journal*, 2020b.

K. Zheng, W. Mou, and L. Wang. Collect at once, use effectively: Making non-interactive locally private learning possible. In *ICML*, pp. 4130–4139, 2017.

Q. Zheng, S. Chen, Q. Long, and W. Su. Federated f-differential privacy. In *International Conference on Artificial Intelligence and Statistics*, volume 130, pp. 2251–2259, 2021.

L. Zhu, Z. Liu, and S. Han. Deep leakage from gradients. In *NeurIPS*, volume 32. Curran Associates, Inc., 2019. URL `https://proceedings.neurips.cc/paper/2019/file/60a6c4002cc7b29142def8871531281a-Paper.pdf`.

APPENDIX

A REVISITING RANDOMIZED RESPONSE MECHANISMS FOR LDP

To preserve LDP given the client's input x, we can apply existing RR mechanisms (Wang et al., 2016b; Fanti et al., 2015; Bassily et al., 2017; Kim et al., 2018; Ren et al., 2018; Zheng et al., 2017; Wang & Xu, 2019; Zhao et al., 2019; Gursoy et al., 2019; Alvim et al., 2018; Xiong et al., 2019), such as unary encoding-based approaches (Wang et al., 2017; Erlingsson et al., 2014), hash-based approaches (Wang et al., 2017; Bassily & Smith, 2015; Acharya et al., 2019; Wang et al., 2019c), binary encoding-based approaches (Arachchige et al., 2019; Lyu et al., 2020a), etc. For instance, hash-based approaches such as those of Google RAPPOR (Erlingsson et al., 2014) and OLH (Wang et al., 2017) hash the client's input x onto a bloom filter B of size k using h hash functions. Then, for each client's input x and a bit $i \in B$, RAPPOR creates a perturbed binary value B'_i from B_i with the following randomization probability:

$$B'_i = \begin{cases} 1, & \text{with probability } p/2 \\ 0, & \text{with probability } p/2 \\ B_i, & \text{with probability } 1-p \end{cases} \tag{9}$$

where p is a hyper-parameter. This B' is reused as the basis for all future analysis, learning, and reports on this distinct input x. This approach achieves ϵ_X-LDP, where $\epsilon_X = 2h \ln((1-\frac{p}{2})/\frac{p}{2})$, given that the sensitivity of every bit B_i is $\Delta_{B_i} = 1$ (Erlingsson et al., 2014).

To deal with numerical inputs, e.g., embedded features, generalized RR mechanisms such as Duchi (Duchi & Rogers, 2019; Bhowmick et al., 2018), Piece-wise (Wang et al., 2019a), Hybrid (Wang et al., 2019a), Three-outputs (Zhao et al., 2020b), Suboptimal (Zhao et al., 2020b), LDP-FL (Sun et al., 2021), LATENT (Arachchige et al., 2019), and OME (Lyu et al., 2020a) can be applied.

Asymmetric version of RAPPOR (e.g., (Wang et al., 2017)) designs different randomization probabilities for different inputs. The technique is well-applied in the context of frequency estimation and successfully reduce the communication cost from $O(d)$ to $O(\log n)$ (d is data dimension and n is the number of samples). However, simply applying the mechanism (Wang et al., 2017) does not optimize the model utility and the privacy-utility trade-off when working with machine learning or deep learning models.

Another line of work in LDP is Mironov (2012), which addresses the floating-point arithmetic in implementation of DP applications. The inconsistency between mathematical abstraction of Laplace mechanism with sampling "uniform" floating-point numbers can be exploited to carry out privacy attacks. Floating-point arithmetic is a leaky abstraction, which is ubiquitous in computer systems and is difficult to argue about formally and hard to get right in applications, including all the RR mechanisms.

However, different from the asymmetric version of RAPPOR and the floating-point arithmetic, our proposed f-RR mechanism focuses on mitigating the privacy-utility trade-off. To achieve that, besides the asymmetric nature of the randomization probabilities, our designed f-RR consists of two key components: 1) The bit-aware term $i\%l/l$, which indicates the location of the bit i in each embedded feature associated with the sensitivity of the bit at that location; and 2) The adjustable but bounded α, which takes into account the correlation between privacy loss and the sensitivity of embedded features to mitigate the privacy-utility trade-off and the curse of privacy composition.

The bit-aware property refers to the bits with a more substantial influence on the model utility have smaller randomization probabilities, and vice-versa, under the same privacy protection. By incorporating sensitivities of binary encoding bits into a generalized privacy loss bound, we show that increasing the dimensions of embedded features r, encoding bits l, and model outcomes C marginally affect the randomization probabilities in BitRand under the same privacy budget. This dimension-elastic property is crucial to mitigate the curse of privacy composition by retaining a high value of data transmitted correctly through our randomization given large dimensions of r, l, and C.

Besides the f-RR for protecting the data, we also include the label-RR for protecting the label in our proposed BitRand mechanism, that provides a complete protection for every data sample.

B BitRand Algorithm Pseudo-Code

```
Input: Privacy budget $\epsilon_X$ and $\epsilon_Y$, number of training iterations $T$, learning rate $\eta_t$, binary encoding parameters ($l$ and $m$)
At server side:
Initialize model $\theta^0$
Send the pre-trained model $f^{pre}$ to clients
for $t \in T$ do
    Distribute model parameter $\theta^t$ to each client
    for each client $u$ do
        $\nabla^u_{\theta_t} \leftarrow$ Client-Update($\theta^t$)
    end for
    $\theta_{t+1} = \theta_t - \eta_t \sum_{u \in [1,N]} \nabla^u_{\theta_t} / N$
end for
Output: $(\epsilon_X, \epsilon_Y)$-LDP $\theta$
At client side $u \in [1, N]$:
for each data sample $(x, y_x) \in D_u$ do
    Extracting embedded features: $e_x \leftarrow f^{pre}(x)$
    $v_x \leftarrow \mathit{BinaryEncoding}(e_x)$ # using Eq. 1
    Randomizing $v_x$: $v'_x \leftarrow f$-RR$(v_x)$ with
    $\alpha = \sqrt{\frac{\epsilon_X + rl}{2r \sum_{i=0}^{l-1} \exp(2\epsilon_X \frac{i}{l})}}$ # using Eq. 2
    Randomizing the label $y_x$: $y'_x \leftarrow label$-RR$(y_x)$ with $\beta = \epsilon_Y - \ln(C-1)$ # using Eq. 3
end for
Client-Update($\theta^t$):
    $\nabla^u_{\theta_t} = \sum_{(v'_x, y'_x) \in D'_u} \nabla_{\theta_t} \mathcal{L}(f(e'_x), y'_x) / n_u$
    return $\nabla^u_{\theta_t}$
```

Algorithm 1: BitRand Algorithm in Federated Learning

C Proof of Lemma 1

Proof. Without loss of generality, let us study the l_1-sensitivity of binary encoding bits of a feature's value a in e_x. It is obvious that f-RR(v_a, i) and f-RR$(v_{a|i}, i)$ differs at the bit i in the worst case. The decoded feature of f-RR(v_a, i) is $a' = \mathcal{E}(f\text{-RR}(v_a, i))$.

Let us denote $b_0 b_1 \dots b_{l-1}$ as the binary representation f-RR(v_a, i) of a', where b_0 is the value of a sign bit (i.e., $b_0 = 1$ if $a' >= 0$ and $b_0 = 0$ if $a' < 0$), and $\{b_i\}_{i=1}^{l-1}$ is the value of integer bits and fraction bits. We have a decoding function: $\mathcal{E}(f\text{-RR}(v_a, i)) = (2b_0 - 1)\sum_{i=1}^{l-1} b_i \times 2^{m-i}$. This decoding function is also applicable to $\mathcal{E}(f\text{-RR}(v_{a|i}, i))$. Let us denote $\{b'_i\}_{i=0}^{l-1}$ as the value of the bit i in f-RR$(v_{a|i}, i)$. Following Eq. 4, the l_1-sensitivity of the bit b_i is computed as follows:

- If i is an integer or a fraction bit ($i \in [1, l-1]$), we have: $\Delta_i = \max_{v_a} \| \mathcal{E}(f\text{-RR}(v_a, i)) - \mathcal{E}\big(f\text{-RR}(v_{a|i}, i)\big) \|_1 = \max_{v_a} \|(2b_0 - 1)\Big(\sum_{j=1, j\neq i}^{l-1} b_j 2^{m-j} + b_i 2^{m-i}\Big) - (2b_0 - 1)\Big(\sum_{j=1, j\neq i}^{l-1} b_j 2^{m-j} + b'_i 2^{m-i}\Big)\|_1 = \max_{v_a} \|(2b_0 - 1)(b_i - b'_i)2^{m-i}\|_1 \leq \max_{v_a} \Big(|(2b_0 - 1)|\|b_i - b'_i\|_1 2^{m-i}\Big)$. The Δ_i is maximized when b_i and b'_i are different, and $|2b_0 - 1| = 1$. Therefore, $\Delta_i = 2^{m-i}$.
- If i is the sign bit ($i = 0$), we have: $\Delta_i = \max_{v_a} \| \mathcal{E}(f\text{-RR}(v_a, 0)) - \mathcal{E}\big(f\text{-RR}(v_{a|i}, 0)\big) \|_1 = \max_{v_a} \|(2b_0 - 1)\sum_{i=1}^{l-1} b_i 2^{m-i} - (2b'_0 - 1)\sum_{i=1}^{l-1} b_i 2^{m-i}\|_1 = \max_{v_a} \|(2b_0 - 2b'_0)\sum_{i=1}^{l-1} b_i 2^{m-i}\|_1 \leq \max_{v_a} \Big(|2b_0 - 2b'_0|\|\sum_{i=1}^{l-1} b_i 2^{m-i}\|_1\Big)$. The Δ_i is maximized when b_0 and b'_0 are different and all $\{b_i\}_{i=1}^{l-1} = 1$. Then, $\Delta_i \leq \max_{v_{a|0}} 2\sum_{i=1}^{l-1} 2^{m-i}$. Since $2^1 + \ldots + 2^{l-2} = 2^{l-1} - 2$ (mat), we have: $2\sum_{i=1}^{l-1} 2^{m-i} = 2^{m+1-(l-1)}(2^{l-1} - 1) < 2^{m+1}$. As a result, $\Delta_i = 2^{m+1}$.

From the aforementioned Δ_i of a feature's value in e_x, it is easily expanded to the entire e_x. Since e_x is the concatenation of all l bits of r values in e_x, all bits with the same value of $i\%l$ have the same l_1-sensitivity across rl bits. Therefore, the Δ_i of the sign bit and the integer/fraction bits are 2^{m+1} and $2^{m-i\%l}$, respectively. Consequently, Lemma 1 hold. □

D Proof of Theorem 1

Let us consider a bit i belonging to a feature a, i.e., one of the r features. We denote f-RR(v_a, i) as vector v_a with only the bit i randomized by our f-RR, i.e., all the bits different from i are kept the same in v_a; that is, we only protect the bit i when using the notation f-RR(v_a, i). Given the l_1-sensitivity Δ_i, there always exists a Laplace noise injected into the embedded feature a, i.e.,

$\mathcal{M}(v_a, i) = \mathcal{E}(v_a) + Lap(\Delta_i/\epsilon_i)$, to achieve ϵ_i-LDP in the embedded feature space (Dwork & Roth, 2014). In other words, $\frac{P(\mathcal{M}(v_a,i)=z)}{P(\mathcal{M}(v_{a|i},i)=z)} \leq \exp(\frac{\epsilon_i|\mathcal{E}(v_a)-\mathcal{E}(v_{a|i})|}{\Delta_i})$ where $v_{a|i}$ is the vector that differs from v_a only at the bit i and $z \in Range(\mathcal{M})$.

To ensure that the privacy loss in randomizing the bit i, we need to bound α in Eq. 2 such that $\frac{P(f\text{-RR}(v_a,i)=v_z)}{P(f\text{-RR}(v_{a|i},i)=v_z)} \leq \exp(\frac{\epsilon_i|\mathcal{E}(v_a)-\mathcal{E}(v_{a|i})|}{\Delta_i})$. However, randomizing a binary encoding bit i given v_a and $v_{a|i}$ results in a smaller l_1-distance $|\mathcal{E}(f\text{-RR}(v_a, i)) - \mathcal{E}(f\text{-RR}(v_{a|i}, i))|$ compared with $|\mathcal{E}(v_a) - \mathcal{E}(v_{a|i})|$; since $|\mathcal{E}(f\text{-RR}(v_a, i)) - \mathcal{E}(f\text{-RR}(v_{a|i}, i))| \leq |\mathcal{E}(v_a) - \mathcal{E}(v_{a|i})|$. Thus, we can derive a tighter bound by replacing $|\mathcal{E}(v_a) - \mathcal{E}(v_{a|i})|$ with $|\mathcal{E}(f\text{-RR}(v_a, i)) - \mathcal{E}(f\text{-RR}(v_{a|i}, i))|$. Given $v_a(i)$ is the bit i in v_a, we have

$$\frac{P(f\text{-RR}(v_a, i) = v_z)}{P(f\text{-RR}(v_{a|i}, i) = v_z)} = \frac{P(f\text{-RR}(v_a(i)) = v_z(i))}{P(f\text{-RR}(v_{a|i}(i)) = v_z(i))} \times \prod_{j \neq i, j \in [0, l-1]} \frac{P(v_a(j) = v_z(j))}{P(v_{a|i}(j) = v_z(j))}$$
$$= \frac{P(f\text{-RR}(v_a(i)) = v_z(i))}{P(f\text{-RR}(v_{a|i}(i)) = v_z(i))} \leq \exp(\frac{\epsilon_i|\mathcal{E}(f\text{-RR}(v_a, i)) - \mathcal{E}(f\text{-RR}(v_{a|i}, i))|}{\Delta_i}) \tag{10}$$

However, finding a closed-form solution of α for the tight privacy bound in Eq. 10 is non-trivial, since ϵ_i is intractable. To address this problem, we consider two cases: (1) $\frac{P(f\text{-RR}(v_a(i))=v_z(i))}{P(f\text{-RR}(v_{a|i}(i))=v_z(i))} \geq 1$ and (2) $0 < \frac{P(f\text{-RR}(v_a(i))=v_z(i))}{P(f\text{-RR}(v_{a|i}(i))=v_z(i))} < 1$. Also, since Δ_i captures the magnitude by which a bit i can change the decoding function $\mathcal{E}()$ in the worst case, we have $\frac{\Delta_i}{|\mathcal{E}(f\text{-RR}(v_a,i))-\mathcal{E}(f\text{-RR}(v_{a|i},i))|} \geq 1$.

In the first case, the privacy loss for a bit i can be bounded as follows:

$$\frac{P(f\text{-RR}(v_a(i)) = v_z(i))}{P(f\text{-RR}(v_{a|i}(i)) = v_z(i))} \leq \Big(\frac{P(f\text{-RR}(v_a(i)) = v_z(i))}{P(f\text{-RR}(v_{a|i}(i)) = v_z(i))}\Big)^{\frac{\Delta_i}{|\mathcal{E}(f\text{-RR}(v_a,i))-\mathcal{E}(f\text{-RR}(v_{a|i},i))|}} \leq \exp(\epsilon_i) \tag{11}$$

Since the RR mechanism is independently applied on each bit i in v_a and on every v_a of the r features, Eq. 11 enables us to quantify a *generalized privacy loss bound* of a RR mechanism, in which different bits have different sensitivities to the randomized outcome as follows.

$$\frac{P(f\text{-RR}(v_x) = v_z)}{P(f\text{-RR}(\widetilde{v}_x) = v_z)} = \prod_{i=0}^{rl-1} \frac{P(f\text{-RR}(v_x(i)) = v_z(i))}{P(f\text{-RR}(v_{x|i}(i)) = v_z(i))}$$
$$\leq \prod_{i=0}^{rl-1} \Big(\frac{P(f\text{-RR}(v_x(i)) = v_z(i))}{P(f\text{-RR}(v_{x|i}(i)) = v_z(i))}\Big)^{\frac{\Delta_i}{|\mathcal{E}(f\text{-RR}(v_x,i))-\mathcal{E}(f\text{-RR}(v_{x|i},i))|}} \leq \prod_{i=0}^{rl-1} \exp(\epsilon_i) = \exp(\sum_{i=0}^{rl-1} \epsilon_i) \tag{12}$$

In the second case, the privacy loss for a bit i can be bounded as follows:

$$\frac{P(f\text{-RR}(v_a(i)) = v_z(i))}{P(f\text{-RR}(v_{a|i}(i)) = v_z(i))} \leq \frac{P(f\text{-RR}(v_{a|i}(i)) = v_z(i))}{P(f\text{-RR}(v_a(i)) = v_z(i))}$$
$$\leq \Big(\frac{P(f\text{-RR}(v_{a|i}(i)) = v_z(i))}{P(f\text{-RR}(v_a(i)) = v_z(i))}\Big)^{\frac{\Delta_i}{|\mathcal{E}(f\text{-RR}(v_a,i))-\mathcal{E}(f\text{-RR}(v_{a|i},i))|}} \leq \exp(\epsilon_i) \tag{13}$$

Similarly, we obtain the same result with Eq. 12 in the second case:

$$\frac{P(f\text{-RR}(v_x) = v_z)}{P(f\text{-RR}(\widetilde{v}_x) = v_z)} = \prod_{i=0}^{rl-1} \frac{P(f\text{-RR}(v_x(i)) = v_z(i))}{P(f\text{-RR}(v_{x|i}(i)) = v_z(i))} \leq \prod_{i=0}^{rl-1} \frac{P(f\text{-RR}(v_{x|i}(i)) = v_z(i))}{P(f\text{-RR}(v_x(i)) = v_z(i))}$$
$$\leq \prod_{i=0}^{rl-1} \Big(\frac{P(f\text{-RR}(v_{x|i}(i)) = v_z(i))}{P(f\text{-RR}(v_x(i)) = v_z(i))}\Big)^{\frac{\Delta_i}{|\mathcal{E}(f\text{-RR}(v_x,i))-\mathcal{E}(f\text{-RR}(v_{x|i},i))|}} \leq \prod_{i=0}^{rl-1} \exp(\epsilon_i) = \exp(\sum_{i=0}^{rl-1} \epsilon_i) \tag{14}$$

Consequently, Theorem 1 holds.

E Proof of Theorem 2

To ensure that the privacy loss in randomizing the bit i is bounded by the privacy loss in the embedded space and to take into account different sensitivities of different bits (Theorem 1), we need to find α in Eq. 2 to solve Eq. 12. However, solving Eq. 12 is not straightforward since the privacy budget ϵ_i and the actual l_1-distance $|\mathcal{E}(f\text{-RR}(v_x, i)) - \mathcal{E}(f\text{-RR}(v_{x|i}, i))|$ are intractable. To address this problem, from Eq. 12, we first consider the bit i in all the r embedded features, as follows: $\prod_{a\in[1,r]} \frac{P(f\text{-RR}(v_a(i))=v_z(i))}{P(f\text{-RR}(v_{a|i}(i))=v_z(i))} \leq \exp(\sum_{a\in[1,r]} \frac{\epsilon_i|\mathcal{E}(f\text{-RR}(v_a,i))-\mathcal{E}(f\text{-RR}(v_{a|i},i))|}{\Delta_i}) = \exp(\frac{\epsilon_i}{\Delta_i}\sum_{a\in[1,r]} |\mathcal{E}(f\text{-RR}(v_a, i)) - \mathcal{E}(f\text{-RR}(v_{a|i}, i))|)$. Note that all the bits i, e.g., sign bits, in all the features $a \in [1, r]$ consume the same privacy budget ϵ_i with the same sensitivity Δ_i. The term $\sum_{a\in[1,r]} |\mathcal{E}(f\text{-RR}(v_a, i)) - \mathcal{E}(f\text{-RR}(v_{a|i}, i))|$ can be unbiasedly replaced with $r \times \mathbb{E}|\mathcal{E}(f\text{-RR}(v_a, i)) - \mathcal{E}(f\text{-RR}(v_{a|i}, i))|$ where $\mathbb{E}$ is the expectation of $|\mathcal{E}(f\text{-RR}(v_a, i)) - \mathcal{E}(f\text{-RR}(v_{a|i}, i))|$, since $\lim_{r\to\infty} \mathbb{E}|\mathcal{E}(f\text{-RR}(v_a, i)) - \mathcal{E}(f\text{-RR}(v_{a|i}, i))| = \frac{\sum_{a\in[1,r]} |\mathcal{E}(f\text{-RR}(v_a,i))-\mathcal{E}(f\text{-RR}(v_{a|i},i))|}{r}$. Hence, we have that

$$\prod_{a\in[1,r]} \frac{P(f\text{-RR}(v_a(i)) = v_z(i))}{P(f\text{-RR}(v_{a|i}(i)) = v_z(i))} \leq \exp\Big(\frac{r\epsilon_i \times \mathbb{E}|\mathcal{E}(f\text{-RR}(v_a, i)) - \mathcal{E}(f\text{-RR}(v_{a|i}, i))|}{\Delta_i}\Big)$$

$$\Leftrightarrow \prod_{a\in[1,r]} \Big(\frac{P(f\text{-RR}(v_a(i)) = v_z(i))}{P(f\text{-RR}(v_{a|i}(i)) = v_z(i))}\Big)^{\frac{\Delta_i}{\mathbb{E}|\mathcal{E}(f\text{-RR}(v_a,i))-\mathcal{E}(f\text{-RR}(v_{a|i},i))|}} \leq \exp(r\epsilon_i) \tag{15}$$

Note that, in our work, we consider the worst case is the case that all the bits of two neighboring vectors can be different. The expectation $\mathbb{E}|\mathcal{E}(f\text{-RR}(v_a, i)) - \mathcal{E}(f\text{-RR}(v_{a|i}, i))|$ in Eq. 15 is used to quantify the difference of every two extreme vectors at bit i. Then for the whole vector, it is the sum over the expectation $\mathbb{E}(\cdot)$ of all bits i, as follows: $\sum_{a\in[1,r]} |\mathcal{E}(f\text{-RR}(v_a, i)) - \mathcal{E}(f\text{-RR}(v_{a|i}, i))| = r \times \mathbb{E}|\mathcal{E}(f\text{-RR}(v_a, i)) - \mathcal{E}(f\text{-RR}(v_{a|i}, i))|$. Therefore, the expectation in Eq. 15 does not imply the average-case scenario.

The sum over the expectation $\mathbb{E}(\cdot)$ of all bits i, i.e., $\sum_{a\in[1,r]}\sum_{i\in[0,l-1]} |\mathcal{E}(f\text{-RR}(v_a, i)) - \mathcal{E}(f\text{-RR}(v_{a|i}, i))| = r \times \sum_{i\in[0,l-1]} \mathbb{E}|\mathcal{E}(f\text{-RR}(v_a, i)) - \mathcal{E}(f\text{-RR}(v_{a|i}, i))|$, is used to bound the privacy loss as follows:

$$\begin{aligned}
&\frac{P(f\text{-RR}(v_x) = v_z)}{P(f\text{-RR}(\widetilde{v}_x) = v_z)} \leq \prod_{a\in[1,r]}\prod_{i\in[0,l-1]} \Big(\frac{P(f\text{-RR}(v_a(i)) = v_z(i))}{P(f\text{-RR}(v_{a|i}(i)) = v_z(i))}\Big)^{\frac{\Delta_i}{\mathbb{E}|\mathcal{E}(f\text{-RR}(v_a,i))-\mathcal{E}(f\text{-RR}(v_{a|i},i))|}} \\
&\leq \exp\Big(\sum_{a\in[1,r]}\sum_{i\in[0,l-1]} \frac{\epsilon_i|\mathcal{E}(f\text{-RR}(v_a, i)) - \mathcal{E}(f\text{-RR}(v_{a|i}, i))|}{\Delta_i}\Big) \\
&= \exp\Big(\sum_{i\in[0,l-1]} \frac{\epsilon_i\big(r \times \mathbb{E}|\mathcal{E}(f\text{-RR}(v_a, i)) - \mathcal{E}(f\text{-RR}(v_{a|i}, i))|\big)}{\Delta_i}\Big) \\
&\leq \exp\Big(r\sum_{i\in[0,l-1]} \epsilon_i\Big) \\
&\Leftrightarrow \prod_{i=0}^{rl-1} \Big(\frac{P(f\text{-RR}(v_x(i)) = v_z(i))}{P(f\text{-RR}(v_{x|i}(i)) = v_z(i))}\Big)^{\frac{\Delta_i}{\mathbb{E}|\mathcal{E}(f\text{-RR}(v_x,i))-\mathcal{E}(f\text{-RR}(v_{x|i},i))|}} \leq \exp\Big(\sum_{i=0}^{rl-1} \epsilon_i\Big)
\end{aligned} \tag{16}$$

Now, we need to bound the generalized privacy loss by discovering closed-form solutions of α given the privacy budgets ϵ_X (Theorem 2). In other words, we need to solve Eq. 16 for discovering the closed-form solution of α. To solve it, first we need to calculate $\mathbb{E}|\mathcal{E}(f\text{-RR}(v_x, i)) - \mathcal{E}(f\text{-RR}(v_{x|i}, i))|$. To be more precise, let us denote p_{Xi} and q_{Xi} as p_X and q_X in Eq. 2 for a particular bit i, respectively. Given the worse case of v_x and $v_{x|i}$, there are four possible cases of $|\mathcal{E}(f\text{-RR}(v_x, i)) - \mathcal{E}(f\text{-RR}(v_{x|i}, i))|$:

- If $f\text{-RR}(v_x(i)) = 1$ and $f\text{-RR}(v_{x|i}(i)) = 1$, then $|\mathcal{E}(f\text{-RR}(v_x, i)) - \mathcal{E}(f\text{-RR}(v_{x|i}, i))| = 0$.

- If $f\text{-RR}(v_x(i)) = 0$ and $f\text{-RR}(v_{x|i}(i)) = 0$, then $|\mathcal{E}(f\text{-RR}(v_x, i)) - \mathcal{E}(f\text{-RR}(v_{x|i}, i))| = 0$.
- If $f\text{-RR}(v_x(i)) = 1$ and $f\text{-RR}(v_{x|i}(i)) = 0$, then $|\mathcal{E}(f\text{-RR}(v_x, i)) - \mathcal{E}(f\text{-RR}(v_{x|i}, i))| = \Delta_i$. This happens with the probability $P(f\text{-RR}(v_x(i)) = 1, f\text{-RR}(v_{x|i}(i)) = 0)$. To compute this probability, we use marginal probability and Bayes' theorem, as follows:

$$\begin{aligned}
&P(f\text{-RR}(v_x(i)) = 1, f\text{-RR}(v_{x|i}(i)) = 0) \\
&= P\Big(f\text{-RR}(v_x(i)) = 1, f\text{-RR}(v_{x|i}(i)) = 0, v_x(i) = 1, v_{x|i}(i) = 0\Big) \\
&\quad + P\Big(f\text{-RR}(v_x(i)) = 1, f\text{-RR}(v_{x|i}(i)) = 0, v_x(i) = 0, v_{x|i}(i) = 1\Big) \\
&= P\Big(f\text{-RR}(v_x(i)) = 1 | f\text{-RR}(v_{x|i}(i)) = 0, v_x(i) = 1, v_{x|i}(i) = 0\Big) \\
&\quad \times P(f\text{-RR}(v_{x|i}(i)) = 0 | v_x(i) = 1, v_{x|i}(i) = 0) \\
&\quad \times P(v_x(i) = 1 | v_{x|i}(i) = 0) \times P(v_{x|i}(i) = 0) \\
&\quad + P\Big(f\text{-RR}(v_x(i)) = 1 | f\text{-RR}(v_{x|i}(i)) = 0, v_x(i) = 0, v_{x|i}(i) = 1\Big) \\
&\quad \times P(f\text{-RR}(v_{x|i}(i)) = 0 | v_x(i) = 0, v_{x|i}(i) = 1) \\
&\quad \times P(v_x(i) = 0 | v_{x|i}(i) = 1) \times P(v_{x|i}(i) = 1) \\
&= P\Big(f\text{-RR}(v_x(i)) = 1 | v_x(i) = 1\Big) \\
&\quad \times P(f\text{-RR}(v_{x|i}(i)) = 0 | v_{x|i}(i) = 0) \times P(v_{x|i}(i) = 0) \\
&\quad + P\Big(f\text{-RR}(v_x(i)) = 1 | v_x(i) = 0\Big) \\
&\quad \times P(f\text{-RR}(v_{x|i}(i)) = 0 | v_{x|i}(i) = 1) \times P(v_{x|i}(i) = 1) \\
&= p_{Xi}^2 P(v_{x|i}(i) = 0) + q_{Xi}^2 P(v_{x|i}(i) = 1)
\end{aligned} \tag{17}$$

- If $f\text{-RR}(v_x(i)) = 0$ and $f\text{-RR}(v_{x|i}(i)) = 1$, then $|\mathcal{E}(f\text{-RR}(v_x(i))) - \mathcal{E}(f\text{-RR}(v_{x|i}(i)))| = \Delta_i$. This happens with the probability $P(f\text{-RR}(v_x(i)) = 0, f\text{-RR}(v_{x|i}(i)) = 1)$. To compute this probability, we use marginal probability and Bayes' theorem, as follows:

$$\begin{aligned}
&P(f\text{-RR}(v_x(i)) = 0, f\text{-RR}(v_{x|i}(i)) = 1) \\
&= P\Big(f\text{-RR}(v_x(i)) = 0, f\text{-RR}(v_{x|i}(i)) = 1, v_x(i) = 1, v_{x|i}(i) = 0\Big) \\
&\quad + P\Big(f\text{-RR}(v_x(i)) = 0, f\text{-RR}(v_{x|i}(i)) = 1, v_x(i) = 0, v_{x|i}(i) = 1\Big) \\
&= q_{Xi}^2 P(v_{x|i}(i) = 0) + p_{Xi}^2 P(v_{x|i}(i) = 1)
\end{aligned} \tag{18}$$

Consequently, the expectation $\mathbb{E}|\mathcal{E}(f\text{-RR}(v_x, i)) - \mathcal{E}(f\text{-RR}(v_{x|i}, i))|$ is computed as follows:

$$\begin{aligned}
&\mathbb{E}|\mathcal{E}(f\text{-RR}(v_x, i)) - \mathcal{E}(f\text{-RR}(v_{x|i}, i))| \\
&= \Big(p_{Xi}^2 P(v_{x|i}(i) = 0) + q_{Xi}^2 P(v_{x|i}(i) = 1)\Big)\Delta_i \\
&+ \Big(q_{Xi}^2 P(v_{x|i}(i) = 0) + p_{Xi}^2 P(v_{x|i}(i) = 1)\Big)\Delta_i \\
&= (p_{Xi}^2 + q_{Xi}^2)\Delta_i
\end{aligned} \tag{19}$$

From Eqs. 12, 16, and 19, we have that

$$\begin{aligned}
&\frac{P(f\text{-RR}(v_x) = v_z)}{P(f\text{-RR}(\widetilde{v}_x) = v_z)} \\
&\le \prod_{i=0}^{rl-1} \Big(\frac{P(f\text{-RR}(v_x(i)) = v_z(i))}{P(f\text{-RR}(v_{x|i}(i)) = v_z(i))}\Big)^{\frac{\Delta_i}{\mathbb{E}|\mathcal{E}(f\text{-RR}(v_x, i)) - \mathcal{E}(f\text{-RR}(v_{x|i}, i))|}} \\
&= \prod_{i=0}^{rl-1} \Big(\frac{P(f\text{-RR}(v_x(i)) = 0|v_x(i) = 1)P(f\text{-RR}(v_x(i)) = 1|v_x(i) = 0)}{P(f\text{-RR}(v_x(i)) = 1|v_x(i) = 1)P(f\text{-RR}(v_x(i)) = 0|v_x(i) = 0)}\Big)^{\frac{1}{p_{Xi}^2 + q_{Xi}^2}} \\
&= \prod_{i=0}^{l-1} \Big(\alpha^2 \exp(2\epsilon_X \frac{i}{l})\Big)^{\frac{r}{p_{Xi}^2 + (1-p_{Xi})^2}} \qquad (20)
\end{aligned}$$

Taking the natural logarithm of two sides of Eq. 20:

$$\begin{aligned}
\ln \frac{P(f\text{-RR}(v_x) = v_z)}{P(f\text{-RR}(\widetilde{v}_x) = v_z)} &\le \sum_{i=0}^{l-1} \ln \Big(\alpha^2 \exp(2\epsilon_X \frac{i}{l})\Big)^{\frac{r}{p_{Xi}^2 + (1-p_{Xi})^2}} \\
&= \sum_{i=0}^{l-1} \Big(\frac{r}{p_{Xi}^2 + (1-p_{Xi})^2} \ln \big(\alpha^2 \exp(2\epsilon_X \frac{i}{l})\big)\Big) \qquad (21)
\end{aligned}$$

Let us bound the summation in Eq. 21 using the following inequality:

$$\ln(a) \le a - 1 \text{ for } a > 0 \qquad (22)$$

The proof of Eq. 22 is as follows. Let $a > 0$, we define $h(a) = \ln(a) - a + 1$. We have: $h'(a) = \frac{1}{a} - 1 = 0 \Leftrightarrow a = 1$, and since $h''(a) = -\frac{1}{a^2} < 0, \forall a > 0$, we get the maximal point at $a = 1$. We also have: $\lim_{a \to 0+} h(a) = -\infty = \lim_{a \to \infty} h(a)$. Therefore, $a = 1$ is the global maximal point and than $\forall a > 0, h(a) \le h(a = 1) = 0$, so $\ln(a) - a + 1 \le 0$. Therefore, Eq. 22 does hold.

Note that, to simultaneously satisfy the randomization probabilities $p_X = \frac{1}{1+\alpha \exp(\frac{i\%l}{l}\epsilon_X)} \ge 0$ and $q_X = \frac{\alpha \exp(\frac{i\%l}{l}\epsilon_X)}{1+\alpha \exp(\frac{i\%l}{l}\epsilon_X)} \ge 0$ in Eq. 2, we need to have: *(i)* $1 + \alpha \exp(\frac{i\%l}{l}\epsilon_X) \ge 0$ and *(ii)* $\alpha \exp(\frac{i\%l}{l}\epsilon_X) \ge 0$. Since $\exp(\frac{i\%l}{l}\epsilon_X) \ge 0$ is always true, from *(i)*, $\alpha \ge -\exp(-\frac{i\%l}{l}\epsilon_X)$, and from *(ii)*, $\alpha \ge 0$. Therefore, $\alpha \ge 0$ is necessary to satisfy the condition $p_X \ge 0$ and $q_X \ge 0$. To apply Eq. 22 into Eq. 21, we need to have $a = \alpha^2 \exp(2\epsilon_X \frac{i}{l}) > 0 \Rightarrow \alpha \ne 0$. As a result, we have that

$$\alpha > 0 \qquad (23)$$

Applying Eq. 22 into Eq. 21 where $a = \alpha^2 \exp(2\epsilon_X \frac{i}{l})$:

$$\begin{aligned}
\ln \frac{P(f\text{-RR}(v_x) = v_z)}{P(f\text{-RR}(\widetilde{v}_x) = v_z)} &\le \sum_{i=0}^{l-1} \Big(\frac{r}{p_{Xi}^2 + (1-p_{Xi})^2} \ln \big(\alpha^2 \exp(2\epsilon_X \frac{i}{l})\big)\Big) \\
&\le \sum_{i=0}^{l-1} \frac{r\alpha^2 \exp(2\epsilon_X \frac{i}{l})}{p_{Xi}^2 + (1-p_{Xi})^2} - \sum_{i=0}^{l-1} \frac{r}{p_{Xi}^2 + (1-p_{Xi})^2} \qquad (24)
\end{aligned}$$

To bound the logarithm in Eq. 24, we use: $p_{Xi}^2 + q_{Xi}^2 = p_{Xi}^2 + (1-p_{Xi})^2 = \Big(\frac{1}{1+\alpha \exp(\frac{i\%l}{l}\epsilon_X)}\Big)^2 + \Big(\frac{\alpha \exp(\frac{i\%l}{l}\epsilon_X)}{1+\alpha \exp(\frac{i\%l}{l}\epsilon_X)}\Big)^2 = \frac{1+\Big(\alpha \exp(\frac{i\%l}{l}\epsilon_X)\Big)^2}{\Big(1+\alpha \exp(\frac{i\%l}{l}\epsilon_X)\Big)^2} \le 1$, and $p_{Xi}^2 + (1-p_{Xi})^2 \ge \frac{(p_{Xi}+1-p_{Xi})^2}{2} = \frac{1}{2}$ (In fact,

$\forall a, b : a^2 + b^2 \geq \frac{(a+b)^2}{2} \Leftrightarrow (a-b)^2 \geq 0$, which is true). Note that, from Eq. 19, we have that $\frac{\Delta_i}{\mathbb{E}|\mathcal{E}(f\text{-RR}(v_a, i)) - \mathcal{E}(f\text{-RR}(v_{a|i}, i))|} = \frac{1}{p_{Xi}^2 + q_{Xi}^2} \geq 1$.

Applying these inequalities in Eq. 24, we obtain:

$$\ln \frac{P(f\text{-RR}(v_x) = v_z)}{P(f\text{-RR}(\widetilde{v}_x) = v_z)} \leq \sum_{i=0}^{l-1} \frac{r\alpha^2 \exp(2\epsilon_X \frac{i}{l})}{p_{Xi}^2 + (1 - p_{Xi})^2} - \sum_{i=0}^{l-1} \frac{r}{p_{Xi}^2 + (1 - p_{Xi})^2}$$
$$< \sum_{i=0}^{l-1} 2r\alpha^2 \exp(2\epsilon_X \frac{i}{l}) - \sum_{i=0}^{l-1} r = \sum_{i=0}^{l-1} 2r\alpha^2 \exp(2\epsilon_X \frac{i}{l}) - rl \leq \epsilon_X \tag{25}$$

By solving Eq. 25, we have that

$$\alpha^2 \leq \frac{\epsilon_X + rl}{2r \sum_{i=0}^{l-1} \exp(2\epsilon_X \frac{i}{l})} \Leftrightarrow |\alpha| \leq \sqrt{\frac{\epsilon_X + rl}{2r \sum_{i=0}^{l-1} \exp(2\epsilon_X \frac{i}{l})}} \tag{26}$$

Therefore, from Eqs. 23 and 26, we have that $\forall \alpha : 0 < \alpha \leq \sqrt{\frac{\epsilon_X + rl}{2r \sum_{i=0}^{l-1} \exp(2\epsilon_X \frac{i}{l})}}$, the f-RR mechanism satisfies ϵ_X-LDP. Consequently, Theorem 2 holds.

F Proof of Theorem 3

Proof. We have: $\frac{P(label\text{-RR}(y_x)=z|y_x)}{P(label\text{-RR}(\widetilde{y}_x)=z|\widetilde{y}_x)} \leq \frac{\max P(label\text{-RR}(y_x)=z|y_x)}{\min P(label\text{-RR}(\widetilde{y}_x)=z|\widetilde{y}_x)} = \frac{\frac{\exp(\beta)}{1+\exp(\beta)}}{\frac{1}{(1+\exp(\beta))(C-1)}} = \exp(\beta + \ln(C-1)) \leq \exp(\epsilon_Y) \Leftrightarrow \beta \leq \epsilon_Y - \ln(C-1)$. Consequently, Theorem 3 does hold. □

G *label*-RR and LabelDP comparison

Although our label-RR is inspired by the randomizing probability (Eq. 1, (Ghazi et al., 2021)) in the LabelDP showcased by (Ghazi et al., 2021), there are two major differences between our label-RR and LabelDP discussed next.

(1) We combine f-RR and label-RR to completely protect a data sample. As pointed out in (Busa-Fekete et al., 2021), only protecting the label as in the LabelDP offers a weaker privacy protection than it appears, as the features are sufficiently predictive of the label, obscuring the label is not enough, as a classifier can still be trained on such noisy data; hence, a user experiences privacy loss due to both the public release of the features and the private release of the label.

(2) The RRWithPrior algorithm that is used to guarantee LabelDP requiring publicly available priors and the multi-stage training (LP-MST) illustrating RRWithPrior algorithm cannot be straightforwardly applied to federated learning. In LP-MST algorithm, the dataset is partitioned into subsets, then based on the prior probability to randomize the label and add the data with that randomized label to the training data. These steps are presently applied on centralized training and it has not been show how to be effectively applied in federated learning.

Using the upper bound of β (Theorem 3) results in the same randomizing probabilities between label-RR and LabelDP. For instance, in Eq. 3, $p_Y = \frac{\exp(\beta)}{1+\exp(\beta)} = \frac{\exp(\epsilon_Y - \ln(C-1))}{1+\exp(\epsilon_Y - \ln(C-1))} = \frac{\exp(\epsilon_Y)}{C-1+\exp(\epsilon_Y)}$ and $q_Y = \frac{1}{(1+\exp(\beta))(C-1)} = \frac{1}{C-1+\exp(\epsilon_Y)}$, which is equivalent to Eq. 1 (Ghazi et al., 2021). Therefore, we did not include LabelDP (Ghazi et al., 2021) in comparison.

H Proof of Theorem 4

Proof. We have $\xi_a = \mathbb{E}|\mathcal{E}(f\text{-RR}(v_a)) - \mathcal{E}(v_a)| = \sum_{i \in [0, l-1]} (p_{Xi} \times 0 + q_{Xi} \times \Delta_i) = \sum_{i \in [0, l-1]} q_{Xi} \times \Delta_i$. Therefore, Theorem 4 hold. □

I Corrected Privacy Budget Bounds in LATENT (Arachchige et al., 2019)

In this section, we aim at providing corrected privacy budget bounds for LATENT (Arachchige et al., 2019). LATENT first encodes embedded features e_x into an rl-bit binary vector v_x. Then, each bit $i \in [0, rl-1]$ is randomized by a RR mechanism (i.e., the MOUE algorithm for high sensitivities in Theorem 3.3 (Arachchige et al., 2019)), denoted f-LT, as follows:

$$\forall i \in [0, rl-1] : P(v'_x(i) = 1) = \begin{cases} p_X = \dfrac{1}{1+\alpha}, & \text{if } v_x(i) = 1 \\ q_X = \dfrac{1}{1+\alpha\exp(\frac{\epsilon_X}{rl})}, & \text{if } v_x(i) = 0 \end{cases} \tag{27}$$

From Eq. 27, we also have that $P(v'_x(i) = 0) = 1 - p_X = \frac{\alpha}{1+\alpha}$ if $v_x(i) = 1$, and $P(v'_x(i) = 0) = 1 - q_X = \frac{\alpha\exp(\frac{\epsilon_X}{rl})}{1+\alpha\exp(\frac{\epsilon_X}{rl})}$ if $v_x(i) = 0$.

Theorem 5. *LATENT with the randomization probabilities as in Eq. 27 preserves $\epsilon_{corrected}$-LDP, where $\epsilon_{corrected} = \frac{(1+\alpha)(1+\alpha\exp(\frac{\epsilon_X}{rl}))}{\alpha(1+\exp(\frac{\epsilon_X}{rl}))}\epsilon_X$.*

Proof. Similar to the analysis in **Appendix E**, we obtain the following inequality:

$$\frac{P(f\text{-LT}(v_x) = v_z)}{P(f\text{-LT}(\widetilde{v}_x) = v_z)} \leq \prod_{i=0}^{rl-1}\Big(\frac{P(f\text{-LT}(v_x(i)) = v_z(i))}{P(f\text{-LT}(v_{x|i}(i)) = v_z(i))}\Big)^{\frac{\Delta_i}{\mathbb{E}|\mathcal{E}(f\text{-LT}(v_x,i)) - \mathcal{E}(f\text{-LT}(v_{x|i},i))|}} \leq \exp(\epsilon_X) \tag{28}$$

and the expectation $\mathbb{E}|\mathcal{E}(f\text{-LT}(v_x, i)) - \mathcal{E}(f\text{-LT}(v_{x|i}, i))|$ is computed as follows:

$$\begin{aligned}
&\mathbb{E}|\mathcal{E}(f\text{-LT}(v_x, i)) - \mathcal{E}(f\text{-LT}(v_{x|i}, i))| \\
&= \Big(P(f\text{-LT}(v_x, i) = 1 | v_x(i) = 1) \\
&\quad \times P(f\text{-LT}(v_{x|i}, i) = 0 | v_{x|i}(i) = 0) \times P(v_{x|i}(i) = 0) \\
&\quad + P(f\text{-LT}(v_x, i) = 1 | v_x(i) = 0) \\
&\quad \times P(f\text{-LT}(v_{x|i}, i) = 0 | v_{x|i}(i) = 1) \times P(v_{x|i}(i) = 1)\Big)\Delta_i \\
&\quad + \Big(P(f\text{-LT}(v_x, i) = 0 | v_x(i) = 1) \\
&\quad \times P(f\text{-LT}(v_{x|i}, i) = 1 | v_{x|i}(i) = 0) \times P(v_{x|i}(i) = 0) \\
&\quad + P(f\text{-LT}(v_x, i) = 0 | v_x(i) = 0) \\
&\quad \times P(f\text{-LT}(v_{x|i}, i) = 1 | v_{x|i}(i) = 1) \times P(v_{x|i}(i) = 1)\Big)\Delta_i \\
&= \Big(p_{Xi}(1 - q_{Xi})P(v_{x|i}(i) = 0) + q_{Xi}(1 - p_{Xi})P(v_{x|i}(i) = 1) \\
&\quad + (1 - p_{Xi})q_{Xi}P(v_{x|i}(i) = 0) + (1 - q_{Xi})p_{Xi}P(v_{x|i}(i) = 1)\Big)\Delta_i \\
&= \Big(p_{Xi}(1 - q_{Xi}) + q_{Xi}(1 - p_{Xi})\Big)\Delta_i
\end{aligned} \tag{29}$$

Furthermore, we have:

$$p_{Xi}(1 - q_{Xi}) + q_{Xi}(1 - p_{Xi}) = \frac{\alpha(1 + \exp(\frac{\epsilon_X}{rl}))}{(1+\alpha)(1+\alpha\exp(\frac{\epsilon_X}{rl}))} \tag{30}$$

From Eqs. 28-30, we have that

$$\begin{aligned}
&\frac{P(f\text{-LT}(v_x) = v_z)}{P(f\text{-LT}(\widetilde{v}_x) = v_z)} \\
&\leq \prod_{i=0}^{rl-1} \Big(\frac{P(f\text{-LT}(v_x(i)) = v_z(i))}{P(f\text{-LT}(v_{x|i}(i)) = v_z(i))}\Big)^{\frac{\Delta_i}{\mathbb{E}|\mathcal{E}(f\text{-LT}(v_x,i))-\mathcal{E}(f\text{-LT}(v_{x|i},i))|}} \\
&= \prod_{i=0}^{rl-1} \Big(\frac{P(f\text{-LT}(v_x(i)) = 1|v_x(i) = 1)}{P(f\text{-LT}(v_x(i)) = 0|v_x(i) = 1)}\Big)^{\frac{\Delta_i}{(p_{Xi}(1-q_{Xi})+q_{Xi}(1-p_{Xi}))\Delta_i}} \\
&\quad \times \prod_{i=0}^{rl-1} \Big(\frac{P(f\text{-LT}(v_x(i)) = 0|v_x(i) = 0)}{P(f\text{-LT}(v_x(i)) = 1|v_x(i) = 0)}\Big)^{\frac{\Delta_i}{(p_{Xi}(1-q_{Xi})+q_{Xi}(1-p_{Xi}))\Delta_i}} \\
&= \prod_{i=0}^{rl-1} \Big(\exp(\frac{\epsilon_X}{rl})\Big)^{\frac{1}{p_{Xi}(1-q_{Xi})+q_{Xi}(1-p_{Xi})}} \qquad (31)
\end{aligned}$$

Then, from Eq. 31, we have:

$$\epsilon_{corrected} = \ln\Big(\Pi_{i=0}^{rl-1}\big(\exp(\frac{\epsilon_X}{rl})\big)^{\frac{1}{p_{Xi}(1-q_{Xi})+q_{Xi}(1-p_{Xi})}}\Big) = \frac{(1+\alpha)(1+\alpha\exp(\frac{\epsilon_X}{rl}))}{\alpha(1+\exp(\frac{\epsilon_X}{rl}))}\epsilon_X \qquad (32)$$

Consequently, Theorem 5 holds. □

From Theorem 5, we show the proportion $\epsilon_{corrected}/\epsilon_X$ as a function of r in Figure 9a and as a function of l in Figure 9b. Following the experiment settings in LATENT (Arachchige et al., 2019), with the commonly used $\alpha = 7$, when changing $r \in \{10, 100, 1,000, 10,000\}$ with a fixed $l = 10$ (Figure 9a), or when changing $l \in \{5, 10, 20, 100, 1,000\}$ with a fixed $r = 1,000$ (Figure 9b) and under a tight privacy budget $\epsilon_X = 0.1$, the proportion $\epsilon_{corrected}/\epsilon_X$ moderately changes among $[4.57, 4.75]$. In other words, the $\epsilon_{corrected}$ is remarkably larger than ϵ_X, for most r and l values in practice. Unlike LATENT, our mechanism does not suffer from this problem, i.e., in BitRand, $\epsilon_{corrected}/\epsilon_X = 1$, thanks to our bit-aware randomization probabilities for LDP in binary encoding (**Theorem 2**).

J Corrected Privacy Budget Bounds in OME (Lyu et al., 2020a)

In this section, we aim at providing corrected privacy budget bounds for OME. OME first encodes embedded features e_x into an rl-bit binary vector v_x. Then, each bit $i \in [0, rl-1]$ is randomized by the following f-OME mechanism:

$$\forall i \in [0, rl-1] : P(v'_x(i) = 1) = \begin{cases} p_{1X} = \dfrac{\alpha}{1+\alpha}, & \text{if } i \in 2j, v_x(i) = 1 \\ p_{2X} = \dfrac{1}{1+\alpha^3}, & \text{if } i \in 2j+1, v_x(i) = 1 \\ q_X = \dfrac{1}{1+\alpha\exp(\frac{\epsilon_X}{rl})}, & \text{if } \ v_x(i) = 0 \end{cases} \qquad (33)$$

From Eq. 33, we also have that $P(v'_x(i) = 0) = 1 - p_{1X} = \frac{1}{1+\alpha}$ if $v_x(i) = 1$ and $i \in 2j$, $P(v'_x(i) = 0) = 1 - p_{2X} = \frac{\alpha^3}{1+\alpha^3}$ if $v_x(i) = 1$ and $i \in 2j+1$, and $P(v'_x(i) = 0) = 1 - q_X = \frac{\alpha\exp(\frac{\epsilon_X}{rl})}{1+\alpha\exp(\frac{\epsilon_X}{rl})}$ if $v_x(i) = 0$.

Theorem 6. *OME with the randomization probabilities as in Eq. 33 preserves $\epsilon_{corrected}$-LDP, where $\epsilon_{corrected} = (\frac{rl}{Q_1} - \frac{rl}{Q_2})\ln(\alpha) + \frac{\epsilon_X}{2Q_1} + \frac{\epsilon_X}{2Q_2}$ in which $Q_1 = \frac{\alpha}{1+\alpha}\frac{\alpha\exp(\frac{\epsilon_X}{rl})}{1+\alpha\exp(\frac{\epsilon_X}{rl})} + \frac{1}{1+\alpha\exp(\frac{\epsilon_X}{rl})}\frac{1}{1+\alpha}$ and $Q_2 = \frac{1}{1+\alpha^3}\frac{\alpha\exp(\frac{\epsilon_X}{rl})}{1+\alpha\exp(\frac{\epsilon_X}{rl})} + \frac{1}{1+\alpha\exp(\frac{\epsilon_X}{rl})}\frac{\alpha^3}{1+\alpha^3}$.*

Proof. Similar to the analysis in **Appendix E** and **Appendix I**, we obtain:

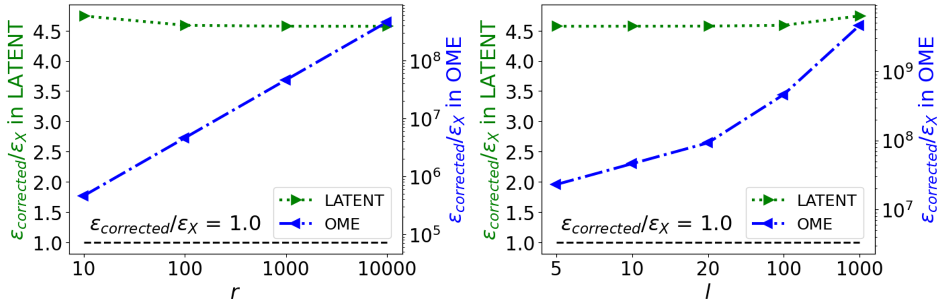

(a) Fixed $\epsilon_X = 0.1, l = 10$

(b) Fixed $\epsilon_X = 0.1, r = 1,000$

Figure 9: Impacts of r and l on $\epsilon_{Corrected}/\epsilon_X$ in LATENT (Arachchige et al., 2019) and OME (Lyu et al., 2020a).

$$\frac{P(f\text{-OME}(v_x) = v_z)}{P(f\text{-OME}(\widetilde{v}_x) = v_z)} \leq \prod_{i=0}^{rl-1} \Big(\frac{P(f\text{-OME}(v_x(i)) = v_z(i))}{P(f\text{-OME}(v_{x|i}(i)) = v_z(i))}\Big)^{\frac{\Delta_i}{\mathbb{E}|\mathcal{E}(f\text{-OME}(v_x,i)) - \mathcal{E}(f\text{-OME}(v_{x|i},i))|}} \leq \exp(\epsilon_X) \tag{34}$$

and the expectation $\mathbb{E}|\mathcal{E}(f\text{-OME}(v_x, i)) - \mathcal{E}(f\text{-OME}(v_{x|i}, i))|$ is computed as follows:

$$\begin{aligned} &\mathbb{E}|\mathcal{E}(f\text{-OME}(v_x, i)) - \mathcal{E}(f\text{-OME}(v_{x|i}, i))| \\ &= \begin{cases} \big(p_{1Xi}(1 - q_{Xi}) + q_{Xi}(1 - p_{1Xi})\big)\Delta_i = Q_1\Delta_i, \text{if } i \in 2j \\ \big(p_{2Xi}(1 - q_{Xi}) + q_{Xi}(1 - p_{2Xi})\big)\Delta_i = Q_2\Delta_i, \text{if } i \in 2j + 1 \end{cases} \end{aligned} \tag{35}$$

where $Q_1 = p_{1Xi}(1 - q_{Xi}) + q_{Xi}(1 - p_{1Xi}) = \frac{\alpha}{1+\alpha} \frac{\alpha \exp(\frac{\epsilon_X}{rl})}{1+\alpha \exp(\frac{\epsilon_X}{rl})} + \frac{1}{1+\alpha \exp(\frac{\epsilon_X}{rl})} \frac{1}{1+\alpha}$,

and $Q_2 = p_{2Xi}(1 - q_{Xi}) + q_{Xi}(1 - p_{2Xi}) = \frac{1}{1+\alpha^3} \frac{\alpha \exp(\frac{\epsilon_X}{rl})}{1+\alpha \exp(\frac{\epsilon_X}{rl})} + \frac{1}{1+\alpha \exp(\frac{\epsilon_X}{rl})} \frac{\alpha^3}{1+\alpha^3}$.

From Eqs. 34 and 35, we have:

$$\begin{aligned} &\frac{P(f\text{-OME}(v_x) = v_z)}{P(f\text{-OME}(\widetilde{v}_x) = v_z)} \\ &\leq \prod_{i=0}^{rl-1} \Big(\frac{P(f\text{-OME}(v_x(i)) = v_z(i))}{P(f\text{-OME}(v_{x|i}(i)) = v_z(i))}\Big)^{\frac{\Delta_i}{\mathbb{E}|\mathcal{E}(f\text{-OME}(v_x,i)) - \mathcal{E}(f\text{-OME}(v_{x|i},i))|}} \\ &= \prod_{i\in 2j} \Big(\frac{P(f\text{-OME}(v_x(i)) = 1|v_x(i) = 1)P(f\text{-OME}(v_x(i)) = 0|v_x(i) = 0)}{P(f\text{-OME}(v_x(i)) = 1|v_x(i) = 0)P(f\text{-OME}(v_x(i)) = 0|v_x(i) = 1)}\Big)^{\frac{\Delta_i}{Q_1\Delta_i}} \\ &\times \prod_{i\in 2j+1} \Big(\frac{P(f\text{-OME}(v_x(i)) = 1|v_x(i) = 1)P(f\text{-OME}(v_x(i)) = 0|v_x(i) = 0)}{P(f\text{-OME}(v_x(i)) = 1|v_x(i) = 0)P(f\text{-OME}(v_x(i)) = 0|v_x(i) = 1)}\Big)^{\frac{\Delta_i}{Q_2\Delta_i}} \\ &= \alpha^{\frac{rl}{Q_1} - \frac{rl}{Q_2}} \exp(\frac{\epsilon_X}{2Q_1} + \frac{\epsilon_X}{2Q_2}) \end{aligned} \tag{36}$$

Then, from Eq. 36, we have:

$$\epsilon_{corrected} = \ln\Big(\alpha^{\frac{rl}{Q_1} - \frac{rl}{Q_2}} \exp(\frac{\epsilon_X}{2Q_1} + \frac{\epsilon_X}{2Q_2})\Big) = (\frac{rl}{Q_1} - \frac{rl}{Q_2})\ln(\alpha) + \frac{\epsilon_X}{2Q_1} + \frac{\epsilon_X}{2Q_2} \tag{37}$$

Consequently, Theorem 6 does hold. □

From Theorem 6, we show the proportion $\epsilon_{corrected}/\epsilon_X$ as a function of r in Figure 9a and as a function of l in Figure 9b. Following the experiment settings in OME (Lyu et al., 2020a), with the commonly used $\alpha = 100$, when changing $r \in \{10, 100, 1,000, 10,000\}$ with a fixed $l = 10$ (Figure 9a), or when changing $l \in \{5, 10, 20, 100, 1,000\}$ with a fixed $r = 1,000$ (Figure 9b) and under a tight privacy budget $\epsilon_X = 0.1$, the proportion $\epsilon_{corrected}/\epsilon_X$ significantly changes among $[4.6e + 6, 4.6e + 9]$. In other words, the $\epsilon_{corrected}$ is extremely larger than ϵ_X, for most r and l values in practice. Since $\alpha = 100$ causes the extreme privacy exaggeration, in our experiment, to compare with OME, we use $\alpha = 1$. This value is used in OME (Lyu et al., 2020a) and generates $\epsilon_{corrected}/\epsilon_X \approx 2$, which offers a reasonable range to apply OME in practice. Unlike OME, our mechanism does not suffer from this problem, i.e., in BitRand, $\epsilon_{corrected}/\epsilon_X = 1$, thanks to our bit-aware randomization probabilities for LDP in binary encoding (**Theorem 2**).

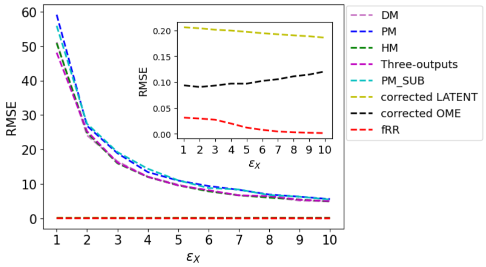

Figure 10: RMSE error comparison as a function of ϵ_X.

K Supplementary Theoretical Results

Setting for Gaussian and Laplace mechanisms. The Gaussian and Laplace mechanisms naturally apply an addition operation, which add noise into the data or embedded features. Therefore, in our analysis of expected error bound comparison for an embedded feature (Figure 3), we add noise into the embedded feature following the Gaussian and Laplace mechanisms. The sensitivity captures the magnitude by which an embedded feature can change in the worst case. In our experiment and analysis, we use $l = 10$ bits in which 1 sign bit, 5 bits for the integer, and 4 bits for the fraction part. Therefore, the maximum the embedded feature can be change, i.e., the sensitivity, is $2\sum_{i=-4}^{4} 2^i$. Note that, we multiply $\sum_{i=-4}^{4} 2^i$ by 2 since when we flip the sign bit, it significantly changes the value of the embedded feature from $-a$ to a in which $a = \sum_{i=-4}^{4} 2^i$.

RMSE error comparison in mean estimation. To investigate how our proposed approach f-RR works with statistical query, we study our f-RR and other baselines with a mean estimation. We created a synthetic data that consists of $N = 1,000$ data samples $\{x_i\}_{i=1}^{N}$, each of them has $d = 768$ dimensions. The mean estimation is calculated over each dimension as $f_j(D) = \frac{1}{N}\sum_{i=1}^{N} x_{ij}$ for $j \in [1, d]$. Root mean square error (RMSE) is used to evaluate the error between the original vector and the randomized/estimated vector. The binary-encoding-based approaches (i.e., f-RR, corrected LATENT, and corrected OME) achieve a significantly small error compared with others. As can be seen in Figure 10, f-RR obtains the smallest error, which further shows the effectiveness of our proposed mechanism.

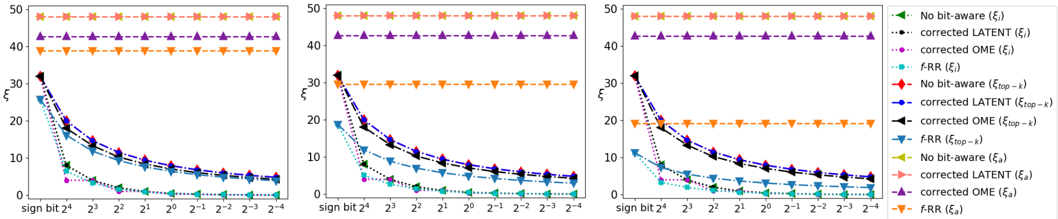

(a) $\epsilon_X = 0.1$ (b) $\epsilon_X = 1.0$ (c) $\epsilon_X = 2.0$

Figure 11: Expected error bound as a function of ϵ_X with fixed r and l.

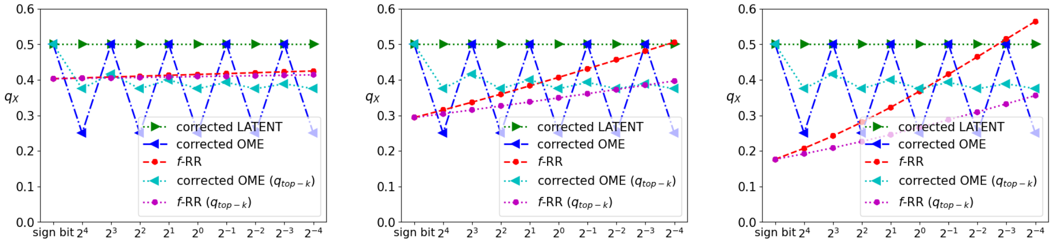

(a) $\epsilon_X = 0.1$ (b) $\epsilon_X = 1.0$ (c) $\epsilon_X = 2.0$

Figure 12: Randomization probability q_X and $q_{top\text{-}k}$, given $l = 10$ and $r = 1,000$.

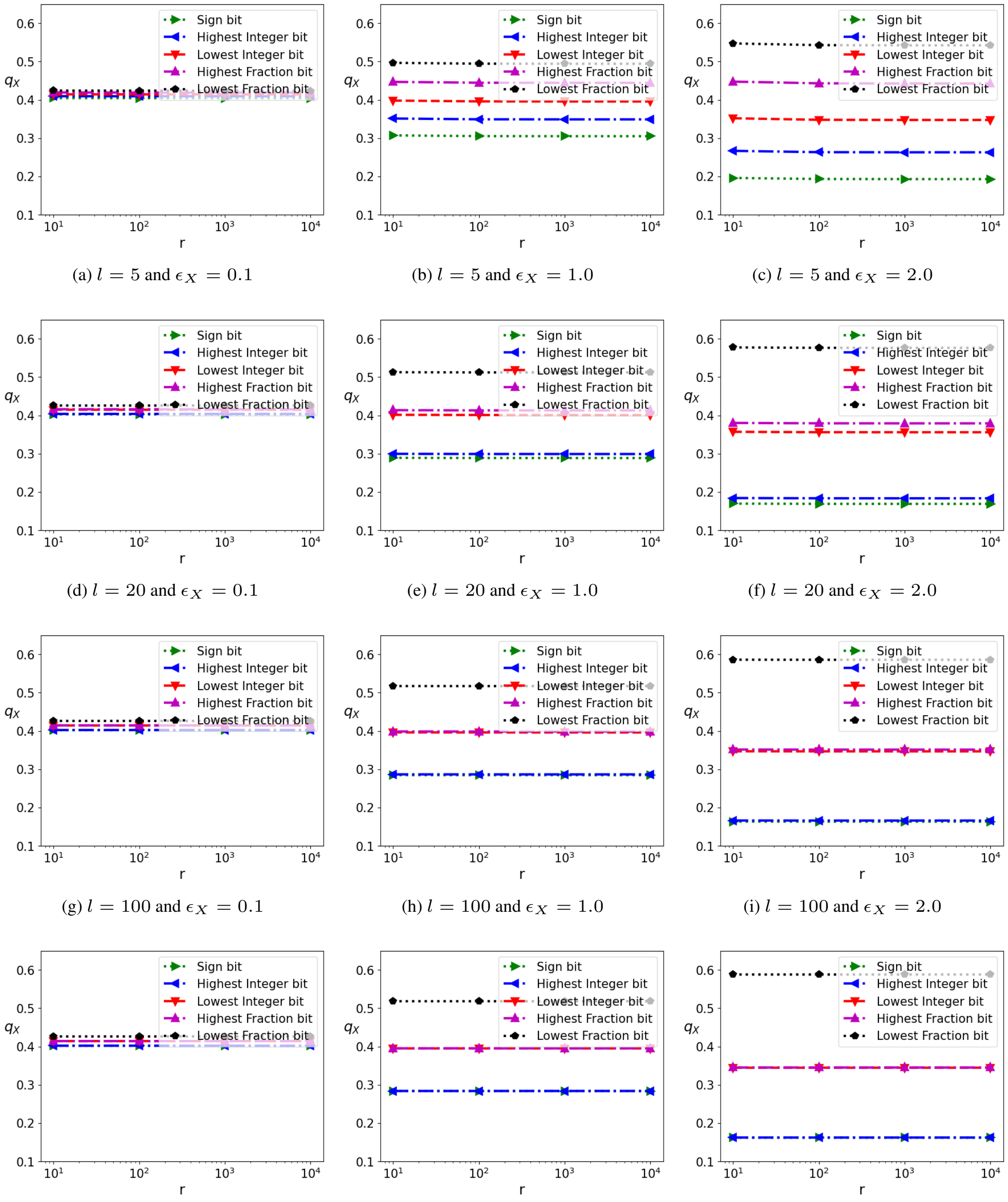

(a) $l = 5$ and $\epsilon_X = 0.1$

(b) $l = 5$ and $\epsilon_X = 1.0$

(c) $l = 5$ and $\epsilon_X = 2.0$

(d) $l = 20$ and $\epsilon_X = 0.1$

(e) $l = 20$ and $\epsilon_X = 1.0$

(f) $l = 20$ and $\epsilon_X = 2.0$

(g) $l = 100$ and $\epsilon_X = 0.1$

(h) $l = 100$ and $\epsilon_X = 1.0$

(i) $l = 100$ and $\epsilon_X = 2.0$

(j) $l = 1,000$ and $\epsilon_X = 0.1$

(k) $l = 1,000$ and $\epsilon_X = 1.0$

(l) $l = 1,000$ and $\epsilon_X = 2.0$

Figure 13: Randomization probability q ($p = 1 - q$) as a function of r with fixed l and ϵ.

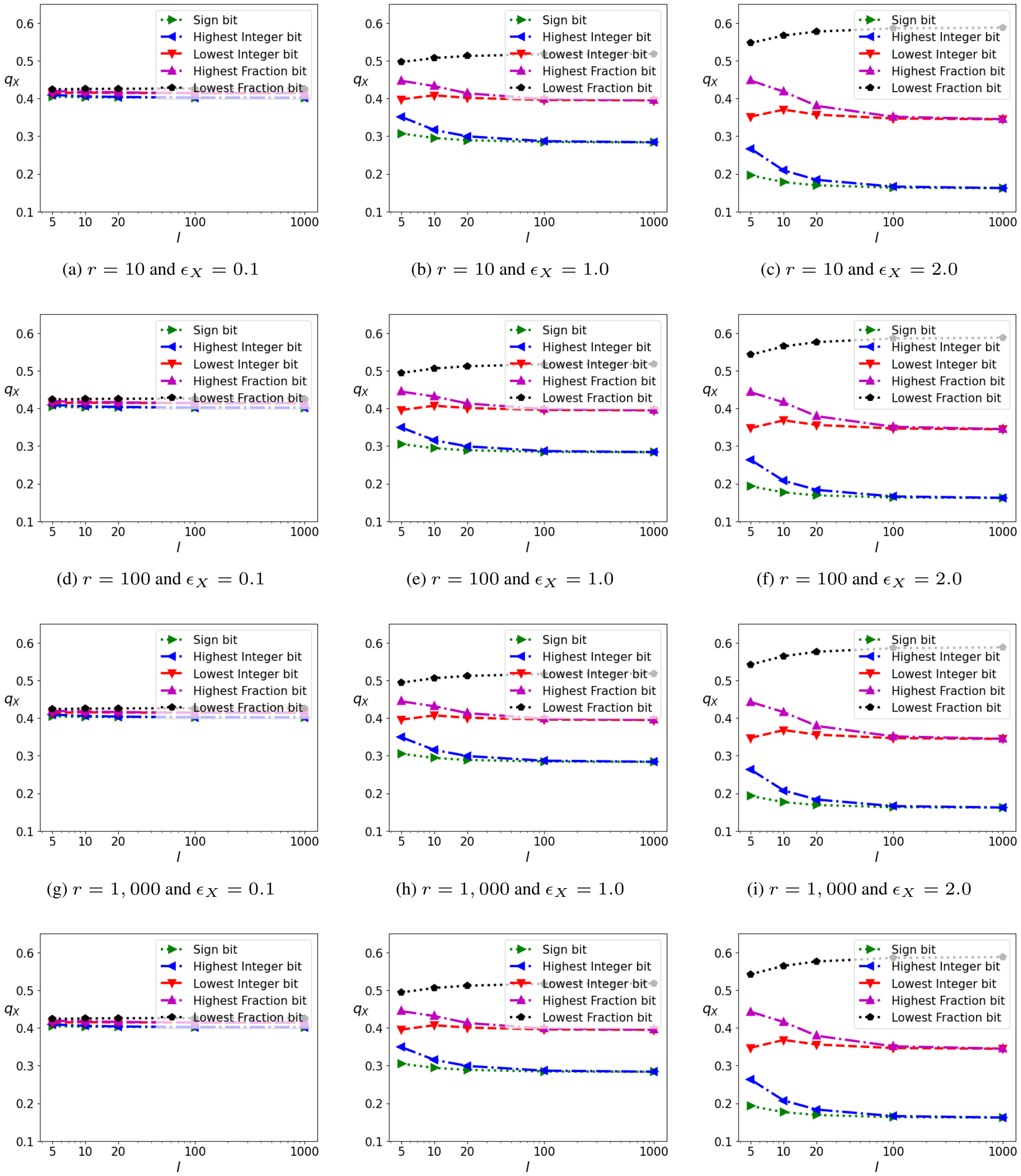

(a) $r = 10$ and $\epsilon_X = 0.1$

(b) $r = 10$ and $\epsilon_X = 1.0$

(c) $r = 10$ and $\epsilon_X = 2.0$

(d) $r = 100$ and $\epsilon_X = 0.1$

(e) $r = 100$ and $\epsilon_X = 1.0$

(f) $r = 100$ and $\epsilon_X = 2.0$

(g) $r = 1,000$ and $\epsilon_X = 0.1$

(h) $r = 1,000$ and $\epsilon_X = 1.0$

(i) $r = 1,000$ and $\epsilon_X = 2.0$

(j) $r = 10,000$ and $\epsilon_X = 0.1$

(k) $r = 10,000$ and $\epsilon_X = 1.0$

(l) $r = 10,000$ and $\epsilon_X = 2.0$

Figure 14: Randomization probability q_X ($p_X = 1 - q_X$) as a function of l with fixed r and ϵ.

L Supplementary Experimental Results

Datasets and Data Processing. We carried out our experiments on two textual datasets and two image datasets, including the AG dataset (Gulli et al., 2012), our collected Security and Exchange Commission (SEC) financial contract dataset, the large-scale celebFaces attributes (CelebA) dataset (Liu et al., 2015), and the Federated Extended MNIST (FEMNIST) dataset (Caldas et al., 2018). The AG dataset is a collection of news articles gathered from more than $2,000$ news sources by (Com). It is categorized into four classes: world, sport, business, and science/technology classes. Our SEC dataset consists of over $1,000$ contract clauses collected from contracts submitted in SEC filings[1]. The CelebA dataset consists of more than $200,000$ celebrity images, each with 40 attributes, e.g., attractive face, big lips, big noses, black hair, etc., which are used as binary classes. The FEMNIST dataset is built by partitioning the images in Extended MNIST (Cohen et al., 2017) based on the writer of the handwritten digits and characters. For data preprocessing, we changed all words in the AG and SEC datasets to lower-case and removed punctuation marks. The breakdown of the datasets is in Table 1.

Table 1: Dataset breakdown.

Dataset	**Train**	**Test**	**Samples/client**	# **classes**
	# samples	# samples	(Average)	
AG	$120,000$	$7,600$	43	4
SEC	$1,021$	134	3	2
CelebA	$155,529$	$19,962$	20	40 (binary)
FEMNIST	$734,033$	$83,818$	227	62

Model Configuration. We use the test accuracy and the test area under the curve (AUC) as evaluation metrics. Models with higher values of test accuracy and AUC are better. We use the BERT-Base (Uncased) pre-trained model (ber; Devlin et al., 2018) to extract embedded features in the AG and SEC datasets. In the CelebA and FEMNIST datasets, we use the ResNet-18 pre-trained model (img; He et al., 2016). Dimension of the extracted embedded features in the AG and SEC datasets is $r = 768$, and in the CelebA and FEMNIST datasets is $r = 512$. For text and image classification tasks, we use two fully connected layers on top of embedded features, each of which consists of $1,500$ hidden neurons and uses a ReLU activation function. The output dimension is corresponding to the number of classes, i.e., 4, 2, 40, and 62 in the AG, SEC, CelebA, and FEMNIST datasets. SGD optimizer with the learning rate is 0.01 in the AG and SEC datasets, 0.1 in the FEMNIST and CelebA datasets.

Experimental setting for anonymization (Sun et al., 2021).

In LDP-FL (Sun et al., 2021), they design a LDP mechanism to perturb the weights at the local client, then each local client applies a split and shuffle mechanism on the weights of local model and sends each weight through an anonymous mechanism to the cloud. The purpose of the shuffling mechanism is to break the linkage among the model weight updates from the same clients and to mix them among updates from other clients, making it harder for the cloud to combine more than one piece of updates to infer more information about any client. Therefore, the key idea of the shuffle mechanism in LDP-FL is to mitigate the privacy degradation by high data dimension and many training/query iterations. In other words, the client anonymity is preserved, and the privacy budget will not accumulate.

When comparing with LDP-FL, we maintain their mechanism' spirits of no privacy accumulation. In the submission, we consider there is no privacy accumulation over the training iterations. It is equivalent to the shuffling step that breaks the linkage among the model weight updates with associated clients. We also used the same randomized response mechanism in the paper, which is Eq. 2 (Sun et al., 2021), to perturb the weight.

In the revision, we added an experiment that do not consider the privacy accumulation over data dimension and training/query iterations. This completely follows the gist of LDP-FL. In addition,

[1] `https://www.sec.gov/edgar.shtml`

the weights we used for LDP-FL. without actual shuffling or splitting can be considered a lossless process, therefore the results we reported here can be counted as an upper-bound result for LDP-FL.

As shown in Table 2, we obtained the slightly higher accuracy of LDP-FL compared with f-RR on the AG dataset. The key component of LDP-FL that helps to reduce the privacy accumulation issue is the shuffling mechanism. However, as pointed out in (Erlingsson et al., 2019), in the real world, it is possible that the anonymizers (i.e., shuffler) can either be compromised or collude with the coordinating server to extract sensitive information. Even though there is a marginally lower trade-off between privacy loss and model utility compared with LDP-FL, the advantage of f-RR is that it perturbs the data only once, then used the perturbed data for training process without facing an extra privacy risk potentially caused by the compromised or colluded anonymizer.

Table 2: Results of LDP-FL without privacy accumulation.

ϵ_X	1	2	3	4	5	6	7	8	9	10
LDP-FL	78.73	82.21	83.25	84.19	84.36	84.22	84.64	84.43	84.31	84.72
f-RR	72.46	79.72	81.42	79.35	81.11	79.84	79.50	80.05	81.20	82.72
Noiseless model	87.59									

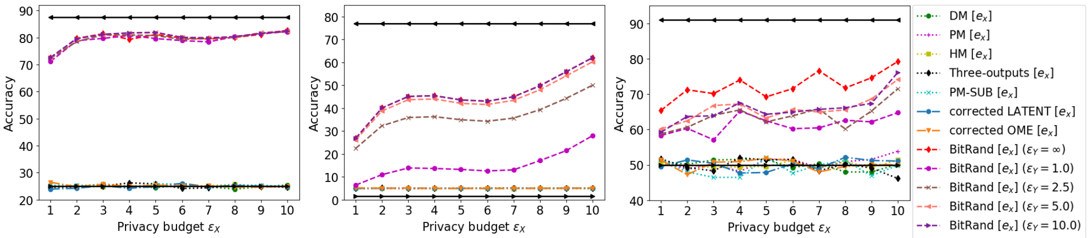

(a) AG (b) FEMNIST (c) SEC

Figure 15: Accuracy of LDP algorithms applied on the embedded features e_x in the AG, SEC, and FEMNIST datasets.

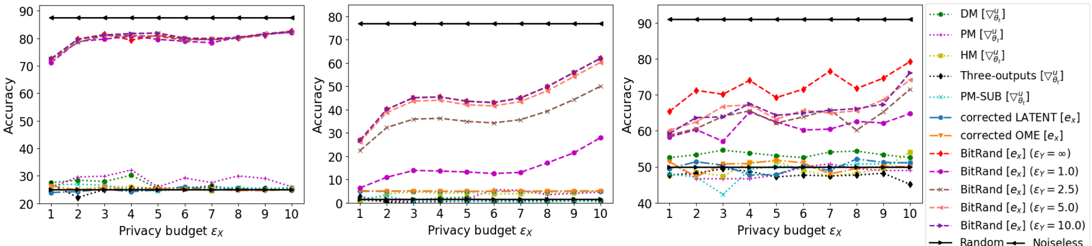

(a) AG (b) FEMNIST (c) SEC

Figure 16: Accuracy of LDP algorithms applied on the gradients $\nabla^u_{\theta_t}$ in the AG, SEC, and FEMNIST datasets.

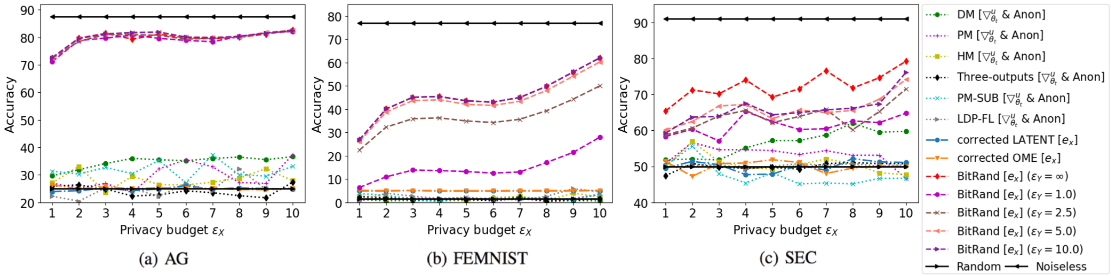

(a) AG (b) FEMNIST (c) SEC

Figure 17: Accuracy of LDP algorithms applied on the gradients $\nabla^u_{\theta_t}$ with the anonymizer (Sun et al., 2021).

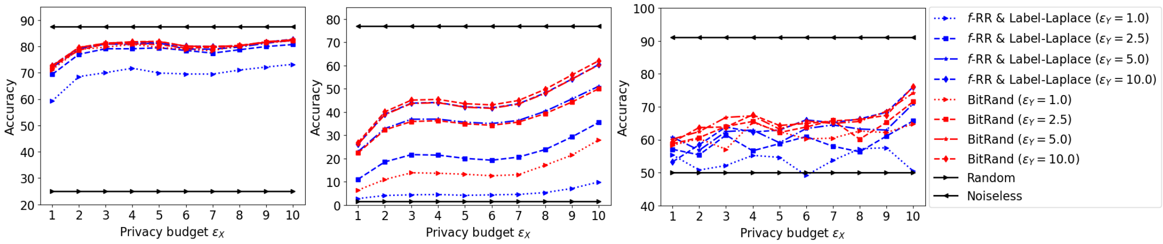

(a) AG (b) FEMNIST (c) SEC

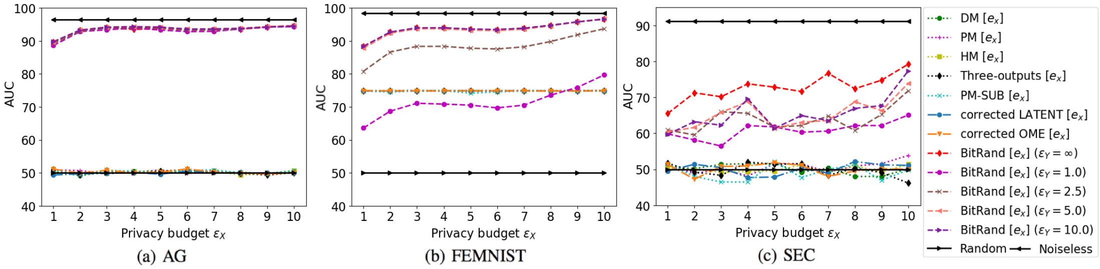

(a) AG (b) FEMNIST (c) SEC

Figure 19: AUC values of LDP algorithms applied on the embedded features e_x in the AG, SEC, and FEMNIST dataset.

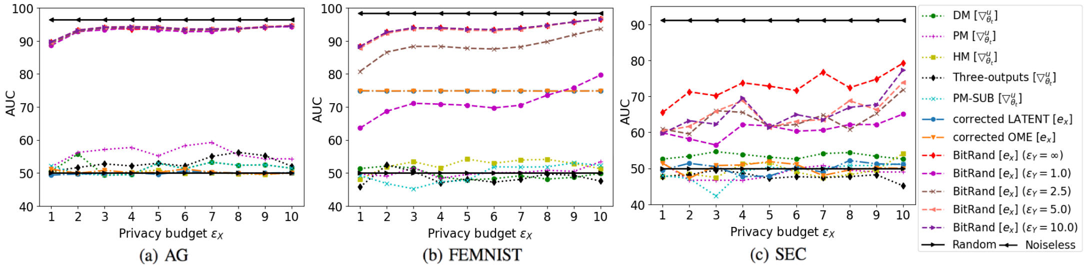

(a) AG (b) FEMNIST (c) SEC

Figure 20: AUC values of LDP algorithms applied on the gradients $\bigtriangledown^u_{\theta_t}$ in the AG, SEC, and FEMNIST datasets.

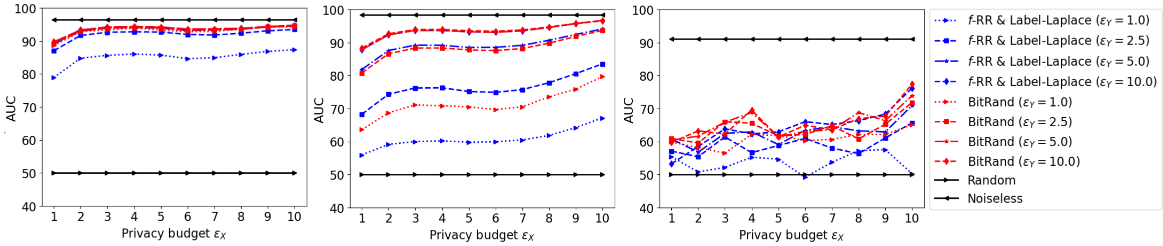

(a) AG (b) FEMNIST (c) SEC

Figure 21: AUC values of each mechanism applied on labels in the AG, SEC, and FEMNIST datasets.

Table 3: AUC values of each algorithm applied on e_x in the CelebA dataset. **Average** is the average of all 40 attributes.

Attribute Algorithm [$\bigtriangledown^{u}_{\theta_t}$ with Anon]		Attractive	Heavy Makeup	High Cheekbones	Male	Mouth Slightly Open	Smiling	Lipstick	**Average**
Noiseless	$\epsilon_X = \infty$	78.05	85.47	76.53	92.77	72.91	79.15	88.85	68.09
DM	$\epsilon_X = 1$	51.96	50.00	50.9	50.12	51.54	51.77	50.63	50.17
	$\epsilon_X = 5$	52.48	50.00	51.04	50.14	51.64	52.08	50.94	50.21
	$\epsilon_X = 10$	52.08	50.00	50.87	50.20	51.91	52.03	50.40	50.19
PM	$\epsilon_X = 1$	51.83	50.00	51.13	50.09	52.22	51.95	50.58	50.20
	$\epsilon_X = 5$	51.67	50.00	50.93	50.39	52.31	51.63	50.59	50.19
	$\epsilon_X = 10$	52.62	50.00	50.98	50.16	52.21	52.02	50.49	50.21
HM	$\epsilon_X = 1$	52.55	50.00	50.56	50.13	51.90	51.53	50.68	50.18
	$\epsilon_X = 5$	52.07	50.00	50.72	50.16	51.65	51.99	50.61	50.18
	$\epsilon_X = 10$	51.86	50.00	50.56	50.09	52.26	52.19	50.63	50.19
Three outputs	$\epsilon_X = 1$	52.57	50.00	50.59	50.19	51.80	51.83	50.62	50.19
	$\epsilon_X = 5$	52.07	50.00	50.75	50.12	52.14	51.66	50.60	50.18
	$\epsilon_X = 10$	51.94	50.00	50.54	50.19	51.44	52.30	50.38	50.17
PM-SUB	$\epsilon_X = 1$	52.44	50.01	51.10	50.13	52.02	51.66	50.74	50.20
	$\epsilon_X = 5$	52.49	50.00	50.87	50.15	52.18	51.64	50.51	50.20
	$\epsilon_X = 10$	51.94	50.00	50.30	50.19	52.02	52.28	50.85	50.19
f-RR and Label -Laplace	$\epsilon_X = 1, \epsilon_Y = 1$	50.00	50.81	50.00	50.03	50.00	50.00	50.00	50.12
	$\epsilon_X = 1, \epsilon_Y = 2.5$	50.00	50.00	50.00	51.39	50.00	50.00	50.00	50.20
	$\epsilon_X = 1, \epsilon_Y = 5$	51.92	50.06	50.31	51.41	50.00	50.01	50.00	50.22
	$\epsilon_X = 5, \epsilon_Y = 1$	50.64	50.00	50.07	50.01	50.00	50.39	50.00	50.21
	$\epsilon_X = 5, \epsilon_Y = 2.5$	50.00	50.23	50.00	49.99	50.00	50.00	50.00	50.10
	$\epsilon_X = 5, \epsilon_Y = 5$	51.87	52.40	50.00	50.00	50.00	50.00	50.00	50.21
	$\epsilon_X = 10, \epsilon_Y = 1$	51.70	50.00	50.00	50.00	50.00	51.03	50.00	50.12
	$\epsilon_X = 10, \epsilon_Y = 2.5$	50.01	50.12	50.00	50.00	50.00	50.05	51.12	50.16
	$\epsilon_X = 10, \epsilon_Y = 5$	50.00	50.00	50.00	50.13	50.01	50.00	50.00	50.21
BitRand	$\epsilon_X = 1, \epsilon_Y = \infty$	59.8	60.65	56.7	64.57	54.56	56.44	64.93	51.86
	$\epsilon_X = 1, \epsilon_Y = 1$	54.52	55.03	53.37	56.99	52.63	53.34	57.43	50.91
	$\epsilon_X = 1, \epsilon_Y = 2.5$	59.08	58.20	55.36	62.02	54.29	55.86	61.91	51.52
	$\epsilon_X = 1, \epsilon_Y = 5$	59.98	60.15	56.28	63.67	54.14	56.91	63.98	51.77
	$\epsilon_X = 5, \epsilon_Y = \infty$	67.15	71.81	60.65	77.91	58.16	61.82	76.15	54.99
	$\epsilon_X = 5, \epsilon_Y = 1$	58.04	59.87	54.24	62.99	54.05	55.67	62.35	51.82
	$\epsilon_X = 5, \epsilon_Y = 2.5$	64.61	67.70	58.78	73.56	56.2	60.04	72.09	53.50
	$\epsilon_X = 5, \epsilon_Y = 5$	67.51	71.41	60.94	77.96	57.82	61.57	76.11	54.82
	$\epsilon_X = 10, \epsilon_Y = \infty$	75.09	81.96	70.14	90.22	65.26	71.76	86.68	63.31
	$\epsilon_X = 10, \epsilon_Y = 1$	61.87	64.88	59.04	68.82	56.8	60.33	67.20	53.84
	$\epsilon_X = 10, \epsilon_Y = 2.5$	71.35	76.69	66.88	84.48	62.74	68.33	81.52	58.16
	$\epsilon_X = 10, \epsilon_Y = 5$	74.45	82.28	69.23	89.88	64.81	71.47	86.38	62.25

Table 4: AUC values of each algorithm applied on the gradients $\bigtriangledown^{u}_{\theta_t}$ with the anonymizer (Sun et al., 2021) in the CelebA dataset.

Algorithm [$\bigtriangledown^{u}_{\theta_t}$ with Anon]	Attribute	Attractive	Heavy Makeup	High Cheekbones	Male	Mouth Slightly Open	Smiling	Lipstick	**Average**
Noiseless	$\epsilon_X = \infty$	78.05	85.47	76.53	92.77	72.91	79.15	88.85	68.09
DM	$\epsilon_X = 1$	43.44	55.86	49.63	65.42	48.86	43.33	60.50	49.85
	$\epsilon_X = 5$	46.94	44.25	49.00	49.68	49.97	51.73	59.24	51.00
	$\epsilon_X = 10$	38.60	40.81	51.87	64.81	49.55	49.05	48.58	50.25
PM	$\epsilon_X = 1$	47.48	62.64	53.94	49.60	50.88	49.07	52.04	50.81
	$\epsilon_X = 5$	53.65	67.99	47.72	44.75	50.13	52.34	43.20	49.72
	$\epsilon_X = 10$	56.85	45.04	52.46	48.42	50.15	49.16	49.81	50.30
HM	$\epsilon_X = 1$	49.61	63.99	52.06	47.27	51.90	48.43	38.25	50.05
	$\epsilon_X = 5$	53.39	42.84	47.26	59.54	53.23	55.21	67.67	51.54
	$\epsilon_X = 10$	44.02	68.26	51.07	54.43	50.17	49.91	44.04	50.42
Three outputs	$\epsilon_X = 1$	54.71	43.89	55.70	55.37	48.46	54.93	43.11	49.99
	$\epsilon_X = 5$	35.45	65.80	50.13	42.53	50.21	45.62	50.36	51.54
	$\epsilon_X = 10$	48.53	46.76	50.03	51.96	53.64	49.57	31.48	49.21
PM-SUB	$\epsilon_X = 1$	41.65	51.61	50.05	63.01	50.35	49.02	51.05	50.29
	$\epsilon_X = 5$	47.62	43.88	50.86	54.82	51.76	53.90	46.81	51.79
	$\epsilon_X = 10$	40.82	74.82	49.86	55.00	54.19	52.39	45.04	51.34
LDP-FL	$\epsilon_X = 1$	41.51	49.43	50.24	33.03	49.01	49.40	53.76	48.71
	$\epsilon_X = 5$	50.35	53.27	51.99	56.76	49.71	50.02	56.31	51.74
	$\epsilon_X = 10$	46.71	46.90	50.11	52.04	47.74	48.50	49.42	50.28
f-RR and Label -Laplace	$\epsilon_X = 1, \epsilon_Y = 1$	50.00	50.81	50.00	50.03	50.00	50.00	50.00	50.12
	$\epsilon_X = 1, \epsilon_Y = 2.5$	50.00	50.00	50.00	51.39	50.00	50.00	50.00	50.20
	$\epsilon_X = 1, \epsilon_Y = 5$	51.92	50.06	50.31	51.41	50.00	50.01	50.00	50.22
	$\epsilon_X = 5, \epsilon_Y = 1$	50.64	50.00	50.07	50.01	50.00	50.39	50.00	50.21
	$\epsilon_X = 5, \epsilon_Y = 2.5$	50.00	50.23	50.00	49.99	50.00	50.00	50.00	50.10
	$\epsilon_X = 5, \epsilon_Y = 5$	51.87	52.40	50.00	50.00	50.00	50.00	50.00	50.21
	$\epsilon_X = 10, \epsilon_Y = 1$	51.70	50.00	50.00	50.00	50.00	51.03	50.00	50.12
	$\epsilon_X = 10, \epsilon_Y = 2.5$	50.01	50.12	50.00	50.00	50.00	50.05	51.12	50.16
	$\epsilon_X = 10, \epsilon_Y = 5$	50.00	50.00	50.00	50.13	50.01	50.00	50.00	50.21
BitRand	$\epsilon_X = 1, \epsilon_Y = \infty$	59.8	60.65	56.7	64.57	54.56	56.44	64.93	51.86
	$\epsilon_X = 1, \epsilon_Y = 1$	54.52	55.03	53.37	56.99	52.63	53.34	57.43	50.91
	$\epsilon_X = 1, \epsilon_Y = 2.5$	59.08	58.20	55.36	62.02	54.29	55.86	61.91	51.52
	$\epsilon_X = 1, \epsilon_Y = 5$	59.98	60.15	56.28	63.67	54.14	56.91	63.98	51.77
	$\epsilon_X = 5, \epsilon_Y = \infty$	67.15	71.81	60.65	77.91	58.16	61.82	76.15	54.99
	$\epsilon_X = 5, \epsilon_Y = 1$	58.04	59.87	54.24	62.99	54.05	55.67	62.35	51.82
	$\epsilon_X = 5, \epsilon_Y = 2.5$	64.61	67.70	58.78	73.56	56.2	60.04	72.09	53.50
	$\epsilon_X = 5, \epsilon_Y = 5$	67.51	71.41	60.94	77.96	57.82	61.57	76.11	54.82
	$\epsilon_X = 10, \epsilon_Y = \infty$	75.09	81.96	70.14	90.22	65.26	71.76	86.68	63.31
	$\epsilon_X = 10, \epsilon_Y = 1$	61.87	64.88	59.04	68.82	56.8	60.33	67.20	53.84
	$\epsilon_X = 10, \epsilon_Y = 2.5$	71.35	76.69	66.88	84.48	62.74	68.33	81.52	58.16
	$\epsilon_X = 10, \epsilon_Y = 5$	74.45	82.28	69.23	89.88	64.81	71.47	86.38	62.25

Table 5: AUC values of each algorithm applied on $\bigtriangledown^{u}_{\theta_t}$ in the CelebA dataset. **Average** is the average of all 40 attributes.

Algorithm [$\bigtriangledown^{u}_{\theta_t}$ with Anon]	Attribute	Attractive	Heavy Makeup	High Cheekbones	Male	Mouth Slightly Open	Smiling	Lipstick	**Average**
Noiseless	$\epsilon_X = \infty$	78.05	85.47	76.53	92.77	72.91	79.15	88.85	68.09
DM	$\epsilon_X = 1$	57.96	29.57	46.45	61.43	50.58	50.9	47.61	47.96
	$\epsilon_X = 5$	59.85	39.72	51.01	53.36	51.15	49.97	32.64	48.62
	$\epsilon_X = 10$	56.33	44.01	50.05	55.19	49.8	52.05	30.79	50.00
PM	$\epsilon_X = 1$	51.87	39.38	49.3	73.24	49.41	48.9	52.99	49.66
	$\epsilon_X = 5$	48.42	40.86	46.84	72.35	50.55	49.52	47.68	50.66
	$\epsilon_X = 10$	49.02	36.59	49.03	59.12	50.39	50.46	53.36	49.22
HM	$\epsilon_X = 1$	46.31	33.84	52.46	42.45	48.33	50.98	48.23	50.41
	$\epsilon_X = 5$	52.39	34.32	52.49	29.79	50.02	48.04	49.90	49.37
	$\epsilon_X = 10$	53.3	49.65	52.23	35.33	50.82	47.69	47.19	50.33
Three outputs	$\epsilon_X = 1$	45.91	63.71	50.16	61.60	51.35	45.39	61.21	50.58
	$\epsilon_X = 5$	35.89	55.43	48.95	55.22	47.60	46.30	58.41	50.39
	$\epsilon_X = 10$	35.03	60.51	49.85	60.69	47.70	43.97	54.05	49.88
PM-SUB	$\epsilon_X = 1$	61.56	63.02	46.78	38.77	52.23	50.38	48.60	48.90
	$\epsilon_X = 5$	58.59	57.14	48.93	31.43	50.54	53.93	51.75	47.93
	$\epsilon_X = 10$	65.09	55.82	47.10	33.13	49.70	51.11	59.87	49.61
f-RR and Label -Laplace	$\epsilon_X = 1, \epsilon_Y = 1$	50.00	50.81	50.00	50.03	50.00	50.00	50.00	50.12
	$\epsilon_X = 1, \epsilon_Y = 2.5$	50.00	50.00	50.00	51.39	50.00	50.00	50.00	50.20
	$\epsilon_X = 1, \epsilon_Y = 5$	51.92	50.06	50.31	51.41	50.00	50.01	50.00	50.22
	$\epsilon_X = 5, \epsilon_Y = 1$	50.64	50.00	50.07	50.01	50.00	50.39	50.00	50.21
	$\epsilon_X = 5, \epsilon_Y = 2.5$	50.00	50.23	50.00	49.99	50.00	50.00	50.00	50.10
	$\epsilon_X = 5, \epsilon_Y = 5$	51.87	52.40	50.00	50.00	50.00	50.00	50.00	50.21
	$\epsilon_X = 10, \epsilon_Y = 1$	51.70	50.00	50.00	50.00	50.00	51.03	50.00	50.12
	$\epsilon_X = 10, \epsilon_Y = 2.5$	50.01	50.12	50.00	50.00	50.00	50.05	51.12	50.16
	$\epsilon_X = 10, \epsilon_Y = 5$	50.00	50.00	50.00	50.13	50.01	50.00	50.00	50.21
BitRand	$\epsilon_X = 1, \epsilon_Y = \infty$	59.8	60.65	56.7	64.57	54.56	56.44	64.93	51.86
	$\epsilon_X = 1, \epsilon_Y = 1$	54.52	55.03	53.37	56.99	52.63	53.34	57.43	50.91
	$\epsilon_X = 1, \epsilon_Y = 2.5$	59.08	58.20	55.36	62.02	54.29	55.86	61.91	51.52
	$\epsilon_X = 1, \epsilon_Y = 5$	59.98	60.15	56.28	63.67	54.14	56.91	63.98	51.77
	$\epsilon_X = 5, \epsilon_Y = \infty$	67.15	71.81	60.65	77.91	58.16	61.82	76.15	54.99
	$\epsilon_X = 5, \epsilon_Y = 1$	58.04	59.87	54.24	62.99	54.05	55.67	62.35	51.82
	$\epsilon_X = 5, \epsilon_Y = 2.5$	64.61	67.70	58.78	73.56	56.2	60.04	72.09	53.50
	$\epsilon_X = 5, \epsilon_Y = 5$	67.51	71.41	60.94	77.96	57.82	61.57	76.11	54.82
	$\epsilon_X = 10, \epsilon_Y = \infty$	75.09	81.96	70.14	90.22	65.26	71.76	86.68	63.31
	$\epsilon_X = 10, \epsilon_Y = 1$	61.87	64.88	59.04	68.82	56.8	60.33	67.20	53.84
	$\epsilon_X = 10, \epsilon_Y = 2.5$	71.35	76.69	66.88	84.48	62.74	68.33	81.52	58.16
	$\epsilon_X = 10, \epsilon_Y = 5$	74.45	82.28	69.23	89.88	64.81	71.47	86.38	62.25